

000 PRISMM-BENCH: A BENCHMARK OF PEER-REVIEW 001 GROUNDED MULTIMODAL INCONSISTENCIES 002

003 **Anonymous authors**
004

005 Paper under double-blind review
006

007 ABSTRACT 008

009 Large Multimodal Models (LMMs) are increasingly applied to scientific research,
010 yet it remains unclear whether they can reliably understand and reason over the
011 multimodal complexity of papers. A central challenge lies in detecting and resolv-
012 ing inconsistencies across text, figures, tables, and equations, issues that are of-
013 ten subtle, domain-specific, and ultimately undermine clarity, reproducibility, and
014 trust. Existing benchmarks overlook this issue, either isolating single modalities
015 or relying on synthetic errors that fail to capture real-world complexity. We intro-
016 duce PRISMM-Bench (*Peer-Review-sourced Inconsistency Set for Multimodal*
017 *Models*), the first benchmark grounded in real reviewer-flagged inconsistencies in
018 scientific papers. Through a multi-stage pipeline of review mining, LLM-assisted
019 filtering and human verification, we curate 384 (before: 262) inconsistencies from
020 353 (before: 242) papers. Based on this set, we design three tasks, namely in-
021 consistency identification, remedy and pair matching, which assess a model’s ca-
022 pacity to detect, correct, and reason over inconsistencies across different modal-
023 ities. Furthermore, to address the notorious problem of *choice-only shortcuts* in
024 multiple-choice evaluation, where models exploit answer patterns without truly
025 understanding the question, we further introduce structured JSON-based answer
026 representations that minimize linguistic biases by reducing reliance on superfi-
027 cial stylistic cues. We benchmark 21 leading LMMs, including large open-weight
028 models (GLM-4.5V 106B, InternVL3 78B) and proprietary models (Gemini 2.5
029 Pro, GPT-5 with high reasoning). Results reveal strikingly low performance (27.8-
030 53.9%) (before: (26.1-54.2%)), underscoring the challenge of multimodal sci-
031 entific reasoning and motivating progress towards trustworthy scientific assistants.
032 We provide the source code and dataset viewer in the appendix, and will release
033 the full source code, dataset, and annotation tool publicly upon acceptance.
034

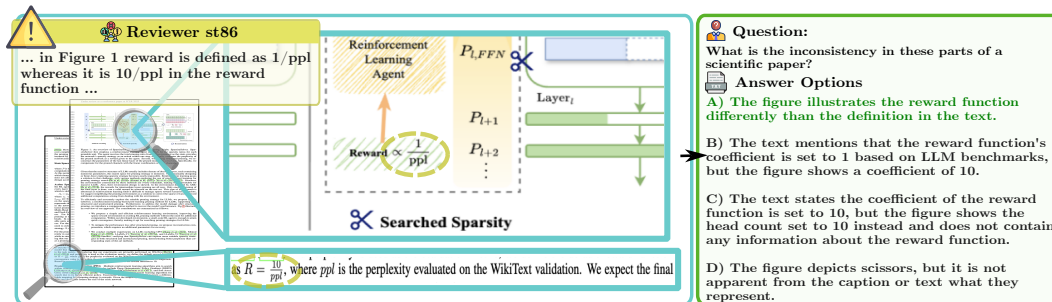


Figure 1: We collect reviewer-flagged inconsistencies in scientific papers and transform them into QA tasks that probe detection, correction, and reasoning over multimodal inconsistencies.

1 INTRODUCTION

Recent advances in Large Multimodal Models (LMMs) have sparked growing interest in their potential to serve as intelligent assistants for scientific research (Eger et al., 2025), supporting tasks

such as figure and chart interpretation (Roberts et al., 2024; Tanasă & Oprea, 2025; Wu et al., 2024), paper summarization (Tan et al., 2025; Saxena et al., 2025; Yu et al., 2025), and error detection (Yang et al., 2025b; Miyai et al., 2024; Alsaif et al., 2024). Yet, a central open question remains: *can LMMs truly reason over the complex multimodal structure of scientific documents?*

A central challenge in this setting is detecting and resolving inconsistencies between text, figures, tables, or equations in scientific papers. These issues are often subtle, arising from copy-paste mistakes, outdated results, or inconsistent notation, and require domain knowledge to detect. Fig. 1 illustrates such a case, where the reward function is defined differently in the figure and the in-line text. Our analysis of ICLR 2025 submissions reveals that 17.0% contained at least one such inconsistency flagged by reviewers. These discrepancies undermine clarity, reproducibility, and ultimately scientific trust.

Existing benchmarks, however, fall short of exposing this. Document QA datasets (Mathew et al., 2021; 2022; Zhu et al., 2022) or standalone scientific visual element tasks focusing on diagrams, charts, or tables (Kafle et al., 2018; Masry et al., 2022; Cheng et al., 2022) miss the multimodal dependencies of scholarly works. Synthetic datasets (Yan et al., 2025) generate artificial errors, but these are often obvious and unrepresentative of real-world complexity. However, constructing such a benchmark of authentic inconsistencies is challenging as these cases are rare, scattered, and labor-intensive to verify, often requiring domain expertise to identify and validate. To address this, we leverage a valuable but underutilized resource - *open peer reviews*, focusing on instances where reviewers flag mismatches across different modalities, such as between text, figures, tables, and equations, thereby providing a natural source of real-world, human-identified inconsistencies.

In this paper, we introduce PRISMM-Bench, a **Peer-Review-sourced Inconsistency Set for Multimodal Models**. Unlike synthetic datasets, PRISMM-Bench captures inconsistencies explicitly flagged by human reviewers in scientific papers on OpenReview. Through a multi-stage pipeline combining large-scale review mining, LLM-assisted filtering, and rigorous human verification, we curate a dataset of 384 (before: 262) inconsistencies across 353 (before: 242) papers submitted to **ICLR 2024 & 2025 (before: ICLR 2025)**, spanning 15 (before: 13) categories of visual-textual and inter-visual mismatches. PRISMM-Bench provides a principled resource for evaluating and improving LMMs, grounded in the real challenges of understanding and verifying scientific papers. Grounded on these recent reviews, we minimize data contamination risk and demonstrate a pipeline with the potential to construct a continuously updated live benchmark. Building on this inconsistency set, we design a benchmark suite of three multiple-choice question (MCQ) tasks: 1) Inconsistency Identification - detect what the inconsistency is; 2) Inconsistency Remedy - determine how to fix the inconsistency; and 3) Inconsistency Pair Match - identify which two elements conflict. Together, these tasks form a tiered framework that evaluates not only a model's ability to spot inconsistencies but also its capacity to propose remedy, and reason over relationships between different modality components.

In MCQ evaluation, a key challenge is models' tendency to rely on linguistic biases in answer choices. Prior work has shown that LLMs often exploit choice-only shortcuts, achieving non-trivial accuracy without reading the question (Chandak et al., 2025; Turner & Kurzeja, 2025; Balepur et al., 2024; Chizhov et al., 2025), and similar effects appear in multimodal MCQs (Chandak et al., 2025). To address this, we propose a novel structured JSON-based answer representation that de-emphasizes stylistic cues and minimizes spurious correlations. Inspired by Das et al. (2014) and Banarescu et al. (2013), our design converts free-form natural language into uniform structured representations that reduce model sensitivity to surface-level patterns. Our user study confirms that this approach suppresses linguistic shortcuts and better aligns models with human reasoning.

We benchmark 21 state-of-the-art LMMs, spanning large open-weight models such as GLM-4.5V 106B (Hong et al., 2025) and InternVL3 78B (Zhu et al., 2025), as well as leading proprietary models including Gemini 2.5 Pro (Comanici et al., 2025) and GPT-5 (OpenAI, 2025). Results show that while large open-weight models achieve around 40% accuracy, even the strongest proprietary models reach just 53.9% (before: 54.2%), underscoring difficulty of the benchmark and limitations of current LMMs.

Our contributions are fourfold: (1) We propose a reviewer-sourced dataset of real multimodal inconsistencies in scientific papers, spanning diverse categories and grounded in peer review. (2) We construct a benchmark suite of three tasks probing detection, correction, and relational reason-

108 ing over these inconsistencies. (3) We are the first to propose JSON-based debiasing method for
 109 MCQ, converting free-form responses into uniform structured representations. (4) We evaluate 21
 110 state-of-the-art LMMs, exposing their current limitations in detecting, understanding and correcting
 111 inconsistencies in scientific papers. The dataset and code for creating the benchmark and evaluating
 112 LMMs will be made publicly available upon acceptance.

2 RELATED WORK

117 **Large Multimodal Models (LMMs).** Large Multimodal Models (LMMs) pair a vision encoder
 118 with a large language model, enabling open-ended reasoning across tasks such as image captioning,
 119 VQA, document understanding, and chart interpretation. Early approaches like BLIP-2 (Li
 120 et al., 2023) and InstructBLIP (Dai et al., 2023) introduced instruction tuning on pre-trained vision-
 121 language models, while the LLaVA series (Liu et al., 2023b;a; Li et al., 2024a) advanced perception
 122 and reasoning via large-scale visual instruction tuning. Several recent studies (Doveh et al., 2024;
 123 Gavrikov et al., 2024; Lin et al., 2024; Huang et al., 2024; Mirza et al., 2025; Hansen et al., 2025;
 124 Mei et al., 2025) have advanced these models by introducing improved training and adaptation
 125 strategies. Recent models extend these capabilities: Qwen-2.5 VL (Bai et al., 2025) offers precise
 126 object localization, dynamic resolution, and agentic tool execution; InternVL3 (Zhu et al., 2025)
 127 improves perception and reasoning through domain-specific pretraining on 3D scenes, GUIs, and
 128 video; Gemma 3 (Team et al., 2025), Ovis 2 (Lu et al., 2025), and GLM 4.5V (Hong et al., 2025)
 129 demonstrate strong performance across diverse multimodal benchmarks. High-resolution variants
 130 such as InternLM XComposer 2.5 (Zhang et al., 2024a) and VILA HD 4K (Shi et al., 2025), enable
 131 detailed perception and document processing. Proprietary models like GPT-5 (OpenAI, 2025) and
 132 Gemini 2.5 Pro (Comanici et al., 2025) set the state-of-the-art on complex multimodal tasks through
 133 large-scale training and enhanced reasoning.

133 These LMMs form the foundation for evaluating multimodal reasoning over scientific documents.
 134 In PRISMM-Bench, we benchmark 21 top-performing models to detect, understand, and correct
 135 real-world inconsistencies in peer-reviewed papers, exposing both their strengths and limitations.

136 **Multimodal Benchmark on Scientific Paper Understanding.** Prior benchmarks often focus on
 137 isolated scientific elements such as diagrams (Kafle et al., 2018; Chaudhry et al., 2020; Kahou
 138 et al., 2018), charts (Masry et al., 2022; Methani et al., 2020), or tables (Cheng et al., 2022; Nan
 139 et al., 2022). Recent datasets like MathVista (Lu et al., 2024), MathVerse (Zhang et al., 2024b),
 140 and ArXivQA (Li et al., 2024b) integrate multiple modalities, but still treat figures and equations
 141 in isolation rather than in full-paper context. Whole-paper QA resources such as PubMedQA (Jin
 142 et al., 2019), BioASQ (Krithara et al., 2023) and QASPER (Dasigi et al., 2021) provide human-
 143 written questions, yet these are mostly abstract-based and limited to yes/no or short-span answers.

144 Closer to our setting, QASA (Lee et al., 2023) provides 1.8K expert-written questions on ML papers,
 145 but remains text-only and does not require reasoning over figures or tables. SPIQA (Pramanick
 146 et al., 2024) introduces multimodal scientific QA, yet the questions are LLM-generated or human-
 147 annotated with an emphasis on information seeking, not grounded on expert reviews that often aim to
 148 critically evaluate scientific findings. SciDQA (Singh et al., 2024) is sourced from reviewer–author
 149 QA pairs, but it remains a text-only LLM benchmark without involving visual elements. In contrast,
 150 PRISMM-Bench is the first benchmark grounded in reviewer-flagged multimodal inconsistencies in
 151 scientific papers. Unlike prior work that isolates figures, tables, or text, our benchmark integrates
 152 visual and textual reasoning within the natural context of full research papers, while grounding tasks
 153 in authentic peer review feedback rather than synthetic or abstract-level annotations.

154 **Understanding of Inconsistencies.** Research on inconsistencies in language models spans prediction
 155 variance across paraphrased queries (Ravichander et al., 2020; Elazar et al., 2021) to factual
 156 inconsistency in summarization and long-form QA. To address the latter, prior work has introduced
 157 QA-based benchmarks (e.g., WikiContradict (Hou et al., 2024)), evaluation metrics (e.g., QAFactE-
 158 val (Fabbri et al., 2022)), and detection methods based on QA (Wang et al., 2020), natural language
 159 inference (Lattimer et al., 2023), or probabilistic reasoning (Marinescu et al., 2025).

160 Closest to our setting, MMIR (Yan et al., 2025) evaluates multimodal models on artificially injected
 161 inconsistencies in materials such as slides and posters. In contrast, PRISMM-Bench introduces real-
 162 world reviewer-flagged inconsistencies in scientific papers. Rather than synthetic perturbations, our

162 benchmark captures authentic challenges faced during scholarly review, spanning textual, visual,
 163 and cross-modal errors, and extends evaluation beyond detection to proposing remedies.
 164

165 **Language Biases in Evaluation Benchmarks.** Multiple-choice evaluation is prone to linguistic
 166 biases, where models exploit surface-level patterns in answer options rather than reasoning over
 167 content. Prior studies show LLMs can achieve high accuracy even without the question, such as in
 168 TruthfulQA (Turner & Kurzeja, 2025), HellaSwag (Zellers et al., 2019), and ARC (Balepur et al.,
 169 2024). For example, Chandak et al. (2025) report 83% accuracy on TruthfulQA v2 using answer
 170 choices alone, with shortcut rates above 70% on HellaSwag. The recent trend of generating distrac-
 171 tors with LLMs (e.g., in MMLU-Pro; Wang et al. (2024a)) can even exacerbate these artifacts.
 172

173 To mitigate such biases, structured representations offer a promising direction. Analogous to au-
 174 thorship obfuscation in stylometry (Chinchor, 1998), structured formats remove stylistic and surface
 175 cues while retaining semantics. Drawing inspiration from FrameNet-based semantic parsing (Das
 176 et al., 2014) and MUC slot filling (Uchendu et al., 2023), PRISMM-Bench introduces JSON-based
 177 answer representations that encode key elements for capturing inconsistencies in scientific papers.
 178 This design reduces artifacts in answer choices and compels models to engage with multimodal
 179 content rather than exploiting linguistic shortcuts.
 180

181 3 PRISMM-BENCH

182 PRISMM-Bench is built through a six-stage pipeline (Fig. 2): (1) review sourcing, (2) LLM-based
 183 review filtering, (3) manual annotation of reviewer-flagged inconsistencies (Sec. 3.1), (4) LMM-
 184 based task generation, (5) manual verification to finalize benchmark tasks (Sec. 3.2), and (6) LLM-
 185 based debiasing to reduce language biases (Sec. 3.3). The evaluation step is introduced in Sec. 3.4.
 186

187 3.1 COLLECTION OF REVIEWER-FLAGGED INCONSISTENCIES

188 To build a benchmark of realistic and authentic inconsistencies, we sourced cases flagged by review-
 189 ers on OpenReview (ope, b), where comments often highlight discrepancies between textual content
 190 and visual or mathematical components, including figures, tables, and equations.
 191

192 **Review Sourcing Strategy.** We collected reviews from ICLR 2024 & 2025 (before: ICLR 2025)
 193 submissions via the OpenReview API v2 (ope, c). To maximize the likelihood that flagged incon-
 194 sistencies persisted in the final public PDFs, we restricted to rejected or withdrawn submissions
 195 without rebuttals.¹ This yielded 18,009 (before: 12,366) reviews (details in App. E.1).
 196

197 **LLM Review Filtering.** As manual screening for all reviews was infeasible, we employed an LLM
 198 for review filtering. Specifically, we used *Mistral Nemo 2407* (Mistral, 2024) with low temperature
 199 settings to summarize reviews and identify potential inconsistency mentions, resulting in a curated
 200 set of 6,056 (before: 5,258) potential inconsistencies spanning 2,458 (before: 3,206; previously
 201 this incorrectly included reviews that did not have inconsistency mentions and has been corrected.)
 202 reviews (prompt details in App. G.1).
 203

204 **Manual Verification.** We performed a manual annotation pass using a custom web-based annotation
 205 tool. The tool presented the annotator with one reviewer-flagged inconsistency at a time, alongside
 206 the corresponding paper in an embedded PDF viewer. Annotators (1) verified whether reviewer
 207 comment described a factual and identifiable inconsistency, and (2) annotated the relevant textual
 208 and/or visual parts of the paper. For visual elements, the annotator selected and cropped regions
 209 from the PDF. For textual elements, they specified the page, line, and content. In addition, each
 210 inconsistency was assigned a category and a brief description in the annotator’s own words. The
 211 tool logged annotations together with the original reviewer’s comment and automatically collected
 212 metadata such as the crop bounding boxes in a structured format. Full details of the annotator
 213 background, annotation tool, captured metadata, annotation criteria and schema are provided in
 214 App. H.
 215

¹Our earlier exploration of review sourcing revealed that most reviewer-flagged inconsistencies were re-
 solved during rebuttal and did not persist in the final versions, motivating the current refined sourcing strategy.

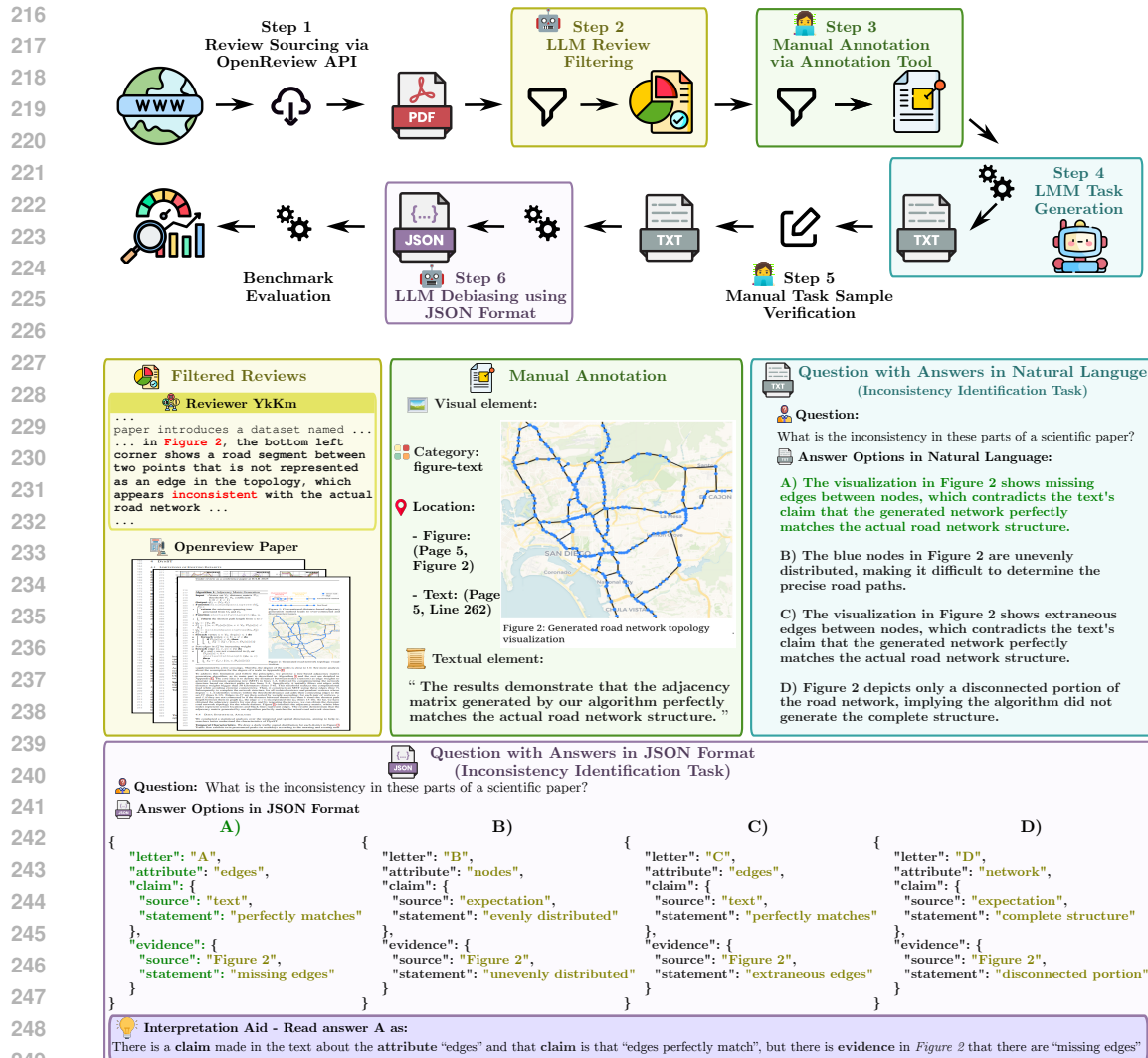


Figure 2: **Pipeline of PRISMM-Bench.** The top row illustrates the six main steps: (1) review sourcing, (2) LLM-based review filtering, and (3) manual annotation of metadata for reviewer-flagged inconsistencies (Sec. 3.1), (4) LMM-based task generation, (5) manual verification to construct benchmark tasks (Sec. 3.2), and (6) LLM-based debiasing to mitigate language biases (Sec. 3.3). The bottom row shows representative outputs at each stage: filtered reviews after step 2, inconsistency annotation after step 3, an example multiple-choice question in natural language after step 4, and its debiased JSON-format counterpart after step 6.

This process produced 384 (before: 262) validated inconsistencies across 353 (before: 242) ICLR submissions. We identified 15 (before: 13) categories of inconsistencies based on the elements involved (distribution shown in Fig. 9). The most common cases were intra-figure inconsistencies (23.7%) (before: figure-text mismatches (24.4%)) and figure-text mismatches (21.9%) (before: intra-figure inconsistencies (24.0%)).

3.2 GENERATION OF BENCHMARK TASKS

From the verified inconsistencies, we constructed three multiple-choice tasks with four options (one correct, three distractors), following the evaluation choice of most recent frontier model releases (Yang et al., 2025a; Liu et al., 2025; Comanici et al., 2025; Team et al., 2024) and benchmarking efforts (Wang et al., 2024b; Zhang et al., 2025; Shabtay et al., 2025). We design the following three multiple-choice tasks.

270 **Inconsistency Identification (*Ident*).** The first task evaluates a model’s ability to recognize inconsistencies within the given paper context, framed by the question: “*What is the inconsistency in these parts of a scientific paper?*” We adopt this generic question style because our preliminary study showed that sample-specific questions (e.g. “*What inconsistency is observed between Figure 2 and the accompanying text regarding the generated road network?*”) reveal the inconsistency content and oversimplify the task (see App. E.4.2 for details).

271 Candidate answers were generated using *Gemini 2.5 Flash* based on inconsistency descriptions and
 272 corresponding multimodal context. The answers were manually refined to ensure (1) the correct
 273 choice captured the inconsistency precisely and (2) the distractors are contextually relevant and
 274 plausible, but incorrect. We show an example of the *Ident* task in Fig. 2.

275 **Inconsistency Remedy (*Remedy*).** This task extends beyond simple detection by requiring models
 276 to how to fix the inconsistency by asking the question “*What action needs to be taken to resolve the*
 277 *inconsistency in these parts of a scientific paper?*” *Gemini 2.5 Flash* was employed to reformulate
 278 the inconsistency statements from *Ident* into specific, actionable remedy formulations. This task
 279 evaluates whether models can propose plausible solutions, rather than merely spotting inconsisten-
 280 cies.

281 **Inconsistency Pair Match (*Match*).** This task is built on a subset of inconsistencies that involve two
 282 distinct visual elements within a paper (192 (before: 135) samples). Given one element as context,
 283 the model must select its inconsistency counterpart from four options. By restricting the task to
 284 visual-visual mismatches, we specifically assess a model’s ability to detect representation errors
 285 without relying on textual cues, simulating the common peer-review challenge of cross-checking
 286 figures and tables for consistency.

287 More details about the task generation process are provided in App. E.4. We provide qualitative
 288 examples of the three tasks in App. B and a dataset viewing tool in the supplementary materials.

296 3.3 ALLEVIATION OF LINGUISTIC BIASES

297 During pilot experiments, we observed that models achieved well above random accuracy even
 298 when the visual context was withheld. For example, *Gemini 2.5 Flash* reached 57.6% accuracy
 299 on the *Ident* task without context (vs. 25% random chance). This indicated that models exploit
 300 linguistic priors and surface patterns in the answer options rather than reasoning over the actual
 301 content. Further analysis showed that factors such as answer length, relative position, and phrasing
 302 contributed to this bias, echoing known challenges in multiple-choice design (Gierl et al., 2017).

303 To combat this bias, we first tried refining the distractors with text manipulation, which proved
 304 insufficient. Therefore, we introduced structured representations that minimize natural language
 305 cues. We designed the *Evidence–Claim JSON* format for the *Ident* task and the *Target–Action JSON*
 306 format for the *Remedy* task. Converting answers into these structured formats using an LLM reduced
 307 *Gemini 2.5 Flash*’s no-context accuracy on the *Ident* task to 34.0%. We manually verified a 20%
 308 subset of the inconsistencies to ensure the semantic fidelity of the JSON-formatted answers. An
 309 example of the *Evidence–Claim JSON* format for the *Ident* task is provided in Fig. 2. Full details on
 310 our debiasing procedure and the structured formats are provided in App. E.4.2.

311 This design choice is further supported by our user study (Sec. 4.3), which reveals that humans rely
 312 minimally on linguistic priors. In contrast, models evaluated on natural language options maintain
 313 high accuracy without context, exposing a fundamental mismatch in evaluation fidelity. By adopting
 314 structured JSON representations, we align model evaluation conditions more closely with human
 315 cognitive constraints, suppressing surface-level shortcuts and enabling a fairer assessment of true
 316 multimodal reasoning.

318 3.4 CONTEXTUAL GRANULARITY IN EVALUATION

319 We evaluate model performance under three levels of contextual granularity, reflecting different
 320 real-world reading conditions and reasoning demands.

321 **Focused Context (*Focused*).** The model is presented only with the minimal necessary components
 322 — an extracted visual element (e.g., cropped figure or table) and/or the precise text passage (e.g.,

324 sentence or paragraph) involved in the inconsistency, as annotated. This setting isolates the key
 325 content, testing the model’s ability to detect inconsistencies with minimal noise.
 326

327 **Page Context (Page).** The model receives a 144 DPI rasterized image of the entire page(s) where
 328 the inconsistency occurs. Visual elements are not pre-cropped, requiring the model to locate and
 329 interpret relevant content within the full page layout. This simulates realistic reading conditions
 330 where inconsistencies must be identified without prior localization.

331 **Document Context (Document).** The model receives the entire scientific paper as a sequence of
 332 page images. To accommodate architectural constraints, we follow MMLongBench-Doc (Ma et al.,
 333 2024) and segment the document into collages: a total of 5 images are fed to the model, each
 334 containing $n_{pages}/5$ pages arranged in a 3-column grid. This setting evaluates the model’s capac-
 335 ity for long-range, cross-page reasoning and document-level grounding. For models with high-
 336 resolution processing constraints, such as *LLaVA Onevision* (7B, 72B), we reduce input to 3 images
 337 with $n_{pages}/3$ pages each to avoid exceeding the context window.

338

339 4 EXPERIMENTS

340

341 4.1 EXPERIMENTAL SETUP

343

344 **Model Selection.** We evaluate 21 LMMs spanning a diverse range of architectures: 16 open-weight
 345 models of varying scales, two specialized high-resolution models, and three proprietary models.
 346 Selection was guided by performance on the Open VLM Leaderboard (ope, a) and the availability
 347 of the latest model versions.

348

349 **Inference Details.** To ensure consistent scoring, we enforced a strict answer format. Prompts at
 350 both the system and user level instructed models to output only the letter corresponding to their
 351 chosen option. For reasoning-enabled models, answers were extracted separately from reasoning
 352 traces, enclosed in `<think></think>` tags, before postprocessing against the ground truth.

353

354 All open-weight models were grouped into three parameter count categories and evaluated with
 355 vLLM v0.10.1 (vll). Experiments were conducted on 4×NVIDIA A100 64GB GPUs with greedy
 356 decoding, except for InternVL3.5 (8B, 38B) which required a temperature of 0.6 for stable reasoning.
 357 Proprietary models were accessed via their official APIs with greedy decoding except *GPT-5*
 (minimal, high) which has a fixed temperature of 1.0.

358

359 Each model was evaluated on all three tasks (*Ident*, *Remedy*, *Match*), and across three contextual
 360 granularity levels (Sec. 3.4). For *Match*, only *Focused Context* was used. This design yields seven
 361 evaluation configurations per model, enabling fine-grained analysis of how model architecture, scale
 362 and input context affect inconsistency detection performance.

363

364 4.2 MAIN RESULTS

365

366 Table 1 summarizes the aggregate performance of all evaluated models. Our results reveal clear
 367 trends in how LMMs handle inconsistency detection and correction.

368

369 **Performance Landscape.** Proprietary models substantially outperform their open-weight counter-
 370 parts. *GPT/5* (high reasoning) reached the highest average performance of 53.9% (before: *Gemini*
 371 2.5 Pro and *GPT-5* (high reasoning) reach the highest average performance of 54.2%). By contrast,
 372 the best open-weight model GLM 4.5V 106B achieves 42.5% (before: 41.9%), matching *GPT-5*
 373 (minimal reasoning) but trailing its high-reasoning variant by 11.4 (before: 12.3) points. These re-
 374 sults underscore the difficulty of the benchmark: even the best-performing models remain far from
 375 the reliability required of automated scientific assistants.

376

377 **Impact of Context and Task Formulation.** Performance drops consistently as context scope ex-
 378 pands. Models achieve their best accuracy in the *Focused* setting but often degrade toward random
 379 chance under *Page* and *Document* inputs, reflecting persistent challenges with distraction and long-
 380 range grounding in dense, multi-page inputs. To rule out input quality effects, we performed an
 381 ablation study on rasterization resolution, confirming our 144 DPI baseline (cf. App. D.1).

378
379
380
381
382
383
384
385
386
387
388
389
390391
392 Table 1: Accuracy (%) of 21 diverse LMMs across three tasks (*Ident*, *Remedy*, *Match*) and three
393 levels of contextual granularity (Sec. 3.4). For *Match*, results are reported only under the *Focused*
394 setting. Best result per task bolded, second best underlined. ^R denotes reasoning models. **This table**
has been updated to include the 122 new data points from ICLR 2024

Model	Params [B]	Focused			Page		Document		Average (960)
		Ident (384)	Remedy (384)	Match (192)	Ident (384)	Remedy (384)	Ident (384)	Remedy (384)	
<i>Small Open-Weight Models (<9B)</i>									
Gemma 3 4B	4.0	27.9	29.9	39.6	25.0	24.7	26.6	27.1	27.8
LLaVA OV 7B	7.0	30.5	28.4	29.7	32.0	28.4	28.1	27.9	29.2
Ovis2 8B	8.0	35.4	29.4	22.4	34.4	27.3	31.8	28.1	30.4
Qwen 2.5 VL 7B	7.0	32.8	31.3	58.9	29.9	29.7	26.8	27.1	31.9
InternVL3 8B	8.0	36.5	29.4	56.3	28.6	27.6	30.7	31.8	32.7
InternVL3.5 8B ^R	8.0	49.5	35.9	45.8	38.3	30.5	36.7	31.0	37.7
<i>Medium Open-Weight Models (9B–38B)</i>									
Gemma 3 27B	27.0	36.2	32.8	59.9	30.7	28.6	31.0	27.3	33.3
Gemma 3 12B	12.0	33.9	30.5	63.5	30.7	25.8	30.7	30.5	32.9
Qwen 2.5 VL 32B	32.0	42.4	37.0	45.8	37.2	34.6	38.3	27.9	37.0
Ovis2 34B	34.0	50.0	41.1	37.0	40.6	36.2	33.3	31.8	38.7
InternVL3 38B	38.0	46.6	38.5	56.8	40.6	35.7	37.0	32.0	39.8
InternVL3.5 38B ^R	38.0	54.4	43.5	50.9	40.9	31.3	33.9	31.5	39.8
<i>Large Open-Weight Models (>38B)</i>									
LLaVA OV 72B	72.0	35.4	30.5	28.1	32.3	28.4	31.5	26.0	30.5
Qwen 2.5 VL 72B	72.0	49.7	37.2	32.8	44.0	33.3	35.4	25.3	37.1
InternVL3 78B	78.0	49.5	39.3	45.3	39.3	33.9	35.9	30.5	38.6
GLM 4.5V 106B ^R	106.0	51.8	43.2	52.1	45.8	35.9	40.9	33.1	42.6
<i>Specialized High-Resolution Models</i>									
InternLM XC 2.5 7B	7.0	28.4	25.3	27.6	29.9	27.1	29.9	28.6	28.2
VILA HD 4K 8B	8.0	31.0	30.7	25.5	30.2	29.2	28.6	28.4	29.4
<i>Proprietary Models</i>									
GPT-5 (minimal) ^R	—	53.6	43.5	63.0	47.1	36.5	40.9	32.8	44.0
Gemini 2.5 Pro ^R	—	65.9	61.2	66.7	54.7	51.8	39.8	36.7	52.8
GPT-5 (high) ^R	—	63.8	54.4	70.3	58.1	51.0	46.9	41.1	53.9

420
421
422
423
424
425
426
427
428
429
430
431

Task formulation also plays a critical role. *Remedy* scores are consistently lower than *Ident*, showing that proposing corrections requires deeper reasoning than only detection. Performance on *Match* varies widely across models: Gemma 3 12B achieves 63.5% (before: 64.4%), rivaling proprietary models, whereas much larger models such as InternVL3 78B lag behind at 45.3% (before: 45.9%). These results suggest that architectural design, not just scale, is critical for relational reasoning.

Model Characteristics. Reasoning-enabled models show benefit. For example, InternVL3.5 8B outperforms its non-reasoning predecessor InternVL3 8B by over 5 percentage points, achieving accuracy comparable to models with nearly nine times more parameters. Turning off chain-of-thought reduces accuracy by up to 14 (before: 19) points (cf. App. D.2), directly confirming the contribution of reasoning. In contrast, high-resolution specialists (VILA HD 4K 8B, InternLM XC 2.5 7B) show little advantage in extended-context settings. More broadly, our results challenge the “bigger is better” paradigm: scaling up parameter counts alone does not guarantee higher performance, with diminishing returns observed from medium- to large-scale models.

Overall, these findings highlight the current limitations of LMMs for scientific document analysis. Future progress will require advances in reasoning architectures to move beyond error detection toward correction, as well as more robust mechanisms for grounding over long, distractive contexts.

4.3 USER STUDY AND LINGUISTIC BIAS ANALYSIS

To complement our benchmark, we conducted a user study to establish a human baseline and quantify *visual reliance* — the extent to which answers depend on genuine multimodal reasoning rather than linguistic shortcuts. While our benchmark uses structured JSON outputs for models, our participants are evaluated on natural language (NL) questions as structured formats are less practical without prior training. To enable direct comparison, we re-evaluated representative LMMs on the same *Ident* task subset using natural language answer options.

Setup. Eight non-author participants with at least PhD-level computer science research experience each answered ten randomly sampled *Ident* task questions: five in *Focused* context and five in *Document* context. For each question, participants first answered without context (question + answer options only), then with context. *Focused* context consisted of cropped images and/or text excerpts; *Document* context contains links to original PDFs. The survey was implemented via a custom web interface (cf. App. F).

Table 2: User Study Results. For each context scope, we report Accuracy (%) for both Natural Language (NL) and JSON answer options. Human performance with NL is shown for reference.

Model	Without Context		Focused Context		Whole Document Context	
	NL	JSON	NL	JSON	NL	JSON
Human	27.5	—	77.5	—	65.0	—
InternVL3.5 8B ^R	49.3	28.4	76.3	47.4	56.8	35.1
InternVL3.5 38B ^R	53.7	25.3	76.3	71.1	70.3	40.5
Qwen 2.5 VL 72B	47.8	38.8	65.8	65.8	43.2	48.6
Gemini 2.5 Pro ^R	70.1	37.3	81.6	65.8	83.8	37.8

Analysis. As shown in Table 2, top models like Gemini 2.5 Pro exceed humans under *Focused Context* (81.6% vs. 77.5%) and *Whole Document Context* (83.8% vs. 65.0%). However, a crucial difference emerges in the *Without Context* condition: LMMs maintain high accuracy (up to 70.1%), whereas human performance drops near chance (27.5%). This indicates that LMMs rely heavily on linguistic regularities that humans cannot exploit. Switching to JSON formatting neutralizes this advantage. Without context, model performance collapses toward human levels (e.g., InternVL3.5 38B drops from 53.7% to 25.3%). With context and JSON-structured answer, LMMs no longer match human NL performance, confirming that linguistic shortcuts inflate perceived model capability.

To quantify how much models and human rely on visual evidence versus linguistic priors, we compute the **Visual Reliance Ratio** R , adapted from the normalized Perceptual Score (Gat et al., 2021):

$$R = \frac{Acc_{with_context} - Acc_{without_context}}{1 - Acc_{without_context}} \quad (1)$$

486
 487 Table 3: Impact of answer representation on without-context performance and visual reliance. Ac-
 488 curacy is reported for the *Ident* task. R is computed according to Eq. 1, using *Focused* context as the
 489 with-context baseline. **This table has been updated to include the 122 new data points from ICLR**
 490 **2024**

Model	Natural Language		JSON	
	Accuracy	R	Accuracy	R
InternVL3.5 8B	45.6	17.1	28.6	29.3
InternVL3.5 38B	52.9	22.5	26.3	38.1
Qwen 2.5 VL 72B	49.7	16.1	36.5	20.8
Gemini 2.5 Pro	61.2	43.8	37.8	45.2

491
 492
 493
 494
 495
 496
 497 Higher R indicates stronger dependence on visual context. Human participants achieve $R = 69.0\%$,
 498 while the top model (InternVL3.5 8B) achieves $R = 53.5\%$, confirming that humans rely more on
 499 visual grounding than current LMMs.
 500

501 **Probing Linguistic Bias.** To confirm this effect generalizes beyond the user study subset, we re-
 502 evaluated the same four representative LMMs on the full *Ident* dataset under both Natural Language
 503 and JSON formats (Table 3). The same pattern holds: under natural language, models achieve in-
 504 flated accuracies without context (e.g. **61.2%** (before: **60.3%**) for Gemini 2.5 Pro) but performance
 505 drops toward chance under JSON. Correspondingly, R increases under JSON for all models, show-
 506 ing that structured outputs suppress linguistic shortcuts and force models to rely more on visual
 507 evidence.
 508

509 **Insights.** Two key conclusions emerge: (1) MCQs with long-form answers in natural language
 510 overstate LMM performance, as models can exploit linguistic regularities imperceptible or irrelevant
 511 to humans. (2) Structured JSON representations mitigate this bias, revealing that even the strongest
 512 LMMs still fall short of human-level visual grounding and rely on surface cues when available.
 513

5 CONCLUSIONS

514 We introduce PRISMM-Bench, a multimodal benchmark for evaluating LMMs on real-world sci-
 515 entific inconsistencies. We show that even top-performing models struggle with cross-modal reason-
 516 ing and long-context grounding, while structured answer formats mitigate linguistic shortcuts. This
 517 work highlights limitations of LMMs as scientific assistants and motivates future improvements in
 518 filtering pipelines, cross-domain datasets, and debiasing strategies for long-form MCQs evaluation.
 519

520 **Limitations.** Our benchmark is limited in scope: it currently focuses on AI-domain papers from
 521 **ICLR 2024 & 2024 (before: ICLR 2025)** and emphasizes rejected submissions to capture unresolved
 522 errors. As a result, both the scale and domain coverage are restricted. Future work should expand to
 523 other fields and venues, and explore inconsistencies that may persist in accepted papers, offering a
 524 broader and more representative testbed.
 525
 526
 527
 528
 529
 530
 531
 532
 533
 534
 535
 536
 537
 538
 539

540 6 ETHICS STATEMENT
541542 This work introduces PRISMM-Bench, a benchmark for evaluating multimodal large language
543 models (MLLMs) on scientific document understanding. In developing the benchmark, we exclusively
544 use publicly available research papers from ICLR 2024 & 2025 (before: ICLR 2025), which are
545 distributed under the Creative Commons Attribution 4.0 (CC-BY 4.0) license. This license explicitly
546 permits redistribution, remixing, and adaptation of the material with proper attribution, and we
547 ensure that all source materials are used in full compliance with these terms.548 Our study also includes a small-scale user study to establish a human baseline. All participants were
549 experienced researchers, voluntarily consented to take part, and no personally identifying information
550 was collected or reported. The study design posed no foreseeable risks to participants and did
551 not involve vulnerable populations.552 We recognize that benchmarks can influence the direction of future model development. While
553 PRISMM-Bench may highlight weaknesses in existing systems, it is not intended to facilitate mis-
554 use, such as adversarial attacks on models, but rather to promote more robust and trustworthy sci-
555 entific document analysis. We release the benchmark with the goal of supporting transparent, repro-
556 ducible, and ethical research, in line with the ICLR Code of Ethics.557 No conflicts of interest, sensitive data, or privacy concerns arise in this work.
558559 560 REFERENCES
561562 Open vlm leaderboard. https://huggingface.co/spaces/open_compass/open_vlm_leaderboard, a.

563

564 Openreview. <https://openreview.net>, b.565 Openreview api v2. <https://docs.openreview.net/reference/api-v2/openapi-definition>, c.

566

567 vllm. <https://docs.vllm.ai/en/v0.10.1/>.

568

569 Khalid M Alsaif, Aiiad A Albeshri, Maher A Khemakhem, and Fathy E Eassa. Multimodal large
570 language model-based fault detection and diagnosis in context of industry 4.0. *Electronics*, 13
571 (24):4912, 2024.572 Shuai Bai, Keqin Chen, Xuejing Liu, Jialin Wang, Wenbin Ge, Sibo Song, Kai Dang, Peng Wang,
573 Shijie Wang, Jun Tang, et al. Qwen2.5-vl technical report. 2025. URL <https://arxiv.org/abs/2502.13923>.

574

575 Nishant Balepur, Abhilasha Ravichander, and Rachel Rudinger. Artifacts or abduction: How do
576 llms answer multiple-choice questions without the question?, 2024. URL <https://arxiv.org/abs/2402.12483>.

577

578 Laura Banarescu, Claire Bonial, Shu Cai, Madalina Georgescu, Kira Griffitt, Ulf Hermjakob, Kevin
579 Knight, Philipp Koehn, Martha Palmer, and Nathan Schneider. Abstract Meaning Represen-
580 tation for sembanking. In Antonio Pareja-Lora, Maria Liakata, and Stefanie Dipper (eds.),
581 *Proceedings of the 7th Linguistic Annotation Workshop and Interoperability with Discourse*,
582 pp. 178–186, Sofia, Bulgaria, August 2013. Association for Computational Linguistics. URL
583 <https://aclanthology.org/W13-2322/>.

584

585 Nikhil Chandak, Shashwat Goel, Ameya Prabhu, Moritz Hardt, and Jonas Geiping. Answer
586 matching outperforms multiple choice for language model evaluation, 2025. URL <https://arxiv.org/abs/2507.02856>.

587

588 Ritwick Chaudhry, Sumit Shekhar, Utkarsh Gupta, Pranav Maneriker, Prann Bansal, and Ajay Joshi.
589 Leaf-qa: Locate, encode & attend for figure question answering. In *Proceedings of the IEEE/CVF*
590 *winter conference on applications of computer vision*, pp. 3512–3521, 2020.

591

592 Zhoujun Cheng, Haoyu Dong, Zhiruo Wang, Ran Jia, Jiaqi Guo, Yan Gao, Shi Han, Jian-Guang
593 Lou, and Dongmei Zhang. Hitab: A hierarchical table dataset for question answering and natural
language generation, 2022. URL <https://arxiv.org/abs/2108.06712>.

594 Nancy A. Chinchor. Overview of MUC-7. In *Seventh Message Understanding Conference (MUC-7): Proceedings of a Conference Held in Fairfax, Virginia, April 29 - May 1, 1998*, 1998. URL
 595 <https://aclanthology.org/M98-1001/>.

596

597 Pavel Chizhov, Mattia Nee, Pierre-Carl Langlais, and Ivan P. Yamshchikov. What the hellaswag?
 598 on the validity of common-sense reasoning benchmarks, 2025. URL <https://arxiv.org/abs/2504.07825>.

599

600

601 Gheorghe Comanici, Eric Bieber, Mike Schaeckermann, Ice Pasupat, Noveen Sachdeva, Inderjit
 602 Dhillon, Marcel Blstein, Ori Ram, Dan Zhang, Evan Rosen, et al. Gemini 2.5: Pushing the
 603 frontier with advanced reasoning, multimodality, long context, and next generation agentic capa-
 604 bilities. 2025. URL <https://arxiv.org/abs/2507.06261>.

605

606 Wenliang Dai, Junnan Li, Dongxu Li, Anthony Tiong, Junqi Zhao, Weisheng Wang, Boyang Li,
 607 Pascale Fung, and Steven Hoi. InstructBLIP: Towards General-purpose Vision-Language Models
 608 with Instruction Tuning. 2023.

609

610 Dipanjan Das, Desai Chen, André F. T. Martins, Nathan Schneider, and Noah A. Smith. Frame-
 611 semantic parsing. *Computational Linguistics*, 40(1):9–56, March 2014. doi: 10.1162/COLI_a-
 612 00163. URL <https://aclanthology.org/J14-1002/>.

613

614 Pradeep Dasigi, Kyle Lo, Iz Beltagy, Arman Cohan, Noah A. Smith, and Matt Gardner. A dataset
 615 of information-seeking questions and answers anchored in research papers, 2021. URL <https://arxiv.org/abs/2105.03011>.

616

617 Sivan Doveh, Shaked Perek, M Jehanzeb Mirza, Amit Alfassy, Assaf Arbelle, Shimon Ullman, and
 618 Leonid Karlinsky. Towards Multimodal In-Context Learning for Vision & Language Models.
 619 *arXiv preprint arXiv:2403.12736*, 2024.

620

621 Steffen Eger, Yong Cao, Jennifer D’Souza, Andreas Geiger, Christian Greisinger, Stephanie Gross,
 622 Yufang Hou, Brigitte Krenn, Anne Lauscher, Yizhi Li, Chenghua Lin, Nafise Sadat Moosavi,
 623 Wei Zhao, and Tristan Miller. Transforming science with large language models: A survey on
 624 ai-assisted scientific discovery, experimentation, content generation, and evaluation, 2025. URL
<https://arxiv.org/abs/2502.05151>.

625

626 Yanai Elazar, Nora Kassner, Shauli Ravfogel, Abhilasha Ravichander, Eduard Hovy, Hinrich
 627 Schütze, and Yoav Goldberg. Measuring and improving consistency in pretrained language mod-
 628 els. *Transactions of the Association for Computational Linguistics*, 9:1012–1031, 2021.

629

630 Alexander R. Fabbri, Chien-Sheng Wu, Wenhao Liu, and Caiming Xiong. Qafacteval: Improved qa-
 631 based factual consistency evaluation for summarization, 2022. URL <https://arxiv.org/abs/2112.08542>.

632

633 Itai Gat, Idan Schwartz, and Alexander Schwing. Perceptual score: What data modalities does your
 634 model perceive?, 2021. URL <https://arxiv.org/abs/2110.14375>.

635

636 Paul Gavrikov, Jovita Lukasik, Steffen Jung, Robert Geirhos, Bianca Lamm, Muhammad Jehanzeb
 637 Mirza, Margret Keuper, and Janis Keuper. Are Vision Language Models Texture or Shape Biased
 638 and Can We Steer Them? *arXiv preprint arXiv:2403.09193*, 2024.

639

640 Mark Gierl, Okan Bulut, Qi Guo, and Xinxin Zhang. Developing, analyzing, and using distractors
 641 for multiple-choice tests in education: A comprehensive review. *Review of Educational Research*,
 642 87:0034654317726529, 08 2017. doi: 10.3102/0034654317726529.

643

644 Jacob Hansen, Wei Lin, Junmo Kang, Muhammad Jehanzeb Mirza, Hongyin Luo, Rogerio Feris,
 645 Alan Ritter, James Glass, and Leonid Karlinsky. Instructify: Demystifying metadata to visual
 646 instruction tuning data conversion. *arXiv preprint arXiv:2505.18115*, 2025.

647

648 Wenyi Hong, Wenmeng Yu, Xiaotao Gu, Guo Wang, Guobing Gan, Haomiao Tang, Jiale Cheng,
 649 Ji Qi, Junhui Ji, Lihang Pan, et al. Glm-4.1 v-thinking: Towards versatile multimodal reasoning
 650 with scalable reinforcement learning. *arXiv e-prints*, pp. arXiv–2507, 2025.

648 Yufang Hou, Alessandra Pascale, Javier Carnerero-Cano, Tigran Tchrakian, Radu Marinescu,
 649 Elizabeth Daly, Inkit Padhi, and Prasanna Sattigeri. Wikicontradict: A benchmark for eval-
 650 uating llms on real-world knowledge conflicts from wikipedia. In A. Globerson, L. Mackey,
 651 D. Belgrave, A. Fan, U. Paquet, J. Tomczak, and C. Zhang (eds.), *Advances in Neural Infor-
 652 mation Processing Systems*, volume 37, pp. 109701–109747. Curran Associates, Inc., 2024.
 653 URL https://proceedings.neurips.cc/paper_files/paper/2024/file/c63819755591ea972f8570beffca6b1b-Paper-Datasets_and_Benchmarks_Track.pdf.

656 Irene Huang, Wei Lin, M Jehanzeb Mirza, Jacob A Hansen, Sivan Doveh, Victor Ion Butoi, Roei
 657 Herzig, Assaf Arbelle, Hilde Kuhene, Trevor Darrel, et al. ConMe: Rethinking Evaluation of
 658 Compositional Reasoning for Modern VLMs. *arXiv preprint arXiv:2406.08164*, 2024.

659 Qiao Jin, Bhuwan Dhingra, Zhengping Liu, William W. Cohen, and Xinghua Lu. Pubmedqa: A
 660 dataset for biomedical research question answering, 2019. URL <https://arxiv.org/abs/1909.06146>.

663 Kushal Kafle, Brian Price, Scott Cohen, and Christopher Kanan. Dvqa: Understanding data visual-
 664 izations via question answering. In *Proceedings of the IEEE conference on computer vision and*
 665 *pattern recognition*, pp. 5648–5656, 2018.

666 Samira Ebrahimi Kahou, Vincent Michalski, Adam Atkinson, Akos Kadar, Adam Trischler, and
 667 Yoshua Bengio. Figureqa: An annotated figure dataset for visual reasoning, 2018. URL <https://arxiv.org/abs/1710.07300>.

670 Anastasia Krithara, Anastasios Nentidis, Konstantinos Bougiatiotis, and Georgios Paliouras.
 671 Bioasq-qa: A manually curated corpus for biomedical question answering. *Scientific Data*, 10
 672 (1):170, 2023.

673 Barrett Lattimer, Patrick CHen, Xinyuan Zhang, and Yi Yang. Fast and accurate factual incon-
 674 sistency detection over long documents. In *Proceedings of the 2023 Conference on Empirical*
 675 *Methods in Natural Language Processing*, pp. 1691–1703. Association for Computational Lin-
 676 *guistics*, 2023. doi: 10.18653/v1/2023.emnlp-main.105. URL <http://dx.doi.org/10.18653/v1/2023.emnlp-main.105>.

678 Yoonjoo Lee, Kyungjae Lee, Sunghyun Park, Dasol Hwang, Jaehyeon Kim, Hong-in Lee, and
 679 Moontae Lee. Qasa: advanced question answering on scientific articles. In *International Confer-
 680 ence on Machine Learning*, pp. 19036–19052. PMLR, 2023.

682 Bo Li, Yuanhan Zhang, Dong Guo, Renrui Zhang, Feng Li, Hao Zhang, Kaichen Zhang, Peiyuan
 683 Zhang, Yanwei Li, Ziwei Liu, and Chunyuan Li. Llava-onevision: Easy visual task transfer,
 684 2024a. URL <https://arxiv.org/abs/2408.03326>.

685 Junnan Li, Dongxu Li, Silvio Savarese, and Steven Hoi. Blip-2: Bootstrapping language-image pre-
 686 training with frozen image encoders and large language models, 2023. URL <https://arxiv.org/abs/2301.12597>.

688 Lei Li, Yuqi Wang, Runxin Xu, Peiyi Wang, Xiachong Feng, Lingpeng Kong, and Qi Liu. Multi-
 689 modal arxiv: A dataset for improving scientific comprehension of large vision-language models,
 690 2024b. URL <https://arxiv.org/abs/2403.00231>.

692 Wei Lin, Muhammad Jehanzeb Mirza, Sivan Doveh, Rogerio Feris, Raja Giryes, Sepp Hochreiter,
 693 and Leonid Karlinsky. Comparison Visual Instruction Tuning. *arXiv preprint arXiv:2406.09240*,
 694 2024.

695 Aixin Liu, Bei Feng, Bing Xue, Bingxuan Wang, Bochao Wu, Chengda Lu, Chenggang Zhao,
 696 Chengqi Deng, Chenyu Zhang, Chong Ruan, et al. Deepseek-v3 technical report. 2025. URL
 697 <https://arxiv.org/abs/2412.19437>.

699 Haotian Liu, Chunyuan Li, Yuheng Li, and Yong Jae Lee. Improved Baselines with Visual Instruc-
 700 tion Tuning. *arXiv:2310.03744*, 2023a.

701 Haotian Liu, Chunyuan Li, Qingyang Wu, and Yong Jae Lee. Visual Instruction Tuning. 2023b.

702 Pan Lu, Hritik Bansal, Tony Xia, Jiacheng Liu, Chunyuan Li, Hannaneh Hajishirzi, Hao Cheng, Kai-
 703 Wei Chang, Michel Galley, and Jianfeng Gao. Mathvista: Evaluating mathematical reasoning
 704 of foundation models in visual contexts, 2024. URL <https://arxiv.org/abs/2310.02255>.

705

706 Shiyin Lu, Yang Li, Yu Xia, Yuwei Hu, Shanshan Zhao, Yanqing Ma, Zhichao Wei, Yinglun Li,
 707 Lunhao Duan, Jianshan Zhao, et al. Ovis2.5 technical report. 2025. URL <https://arxiv.org/abs/2508.11737>.

708

709 Yubo Ma, Yuhang Zang, Liangyu Chen, Meiqi Chen, Yizhu Jiao, Xinze Li, Xinyuan Lu, Ziyu Liu,
 710 Yan Ma, Xiaoyi Dong, et al. Mmlongbench-doc: Benchmarking long-context document under-
 711 standing with visualizations. *Advances in Neural Information Processing Systems*, 37:95963–
 712 96010, 2024.

713

714 Radu Marinescu, Debarun Bhattacharjya, Junkyu Lee, Tigran Tcharkian, Javier Carnerero Cano,
 715 Yufang Hou, Elizabeth Daly, and Alessandra Pascale. Factreacher: A probabilistic approach
 716 to long-form factuality assessment for large language models, 2025. URL <https://arxiv.org/abs/2502.18573>.

717

718 Ahmed Masry, Do Xuan Long, Jia Qing Tan, Shafiq Joty, and Enamul Hoque. Chartqa: A
 719 benchmark for question answering about charts with visual and logical reasoning, 2022. URL
 720 <https://arxiv.org/abs/2203.10244>.

721

722 Minesh Mathew, Dimosthenis Karatzas, and CV Jawahar. Docvqa: A dataset for vqa on document
 723 images. In *Proceedings of the IEEE/CVF winter conference on applications of computer vision*,
 724 pp. 2200–2209, 2021.

725

726 Minesh Mathew, Viraj Bagal, Rubèn Tito, Dimosthenis Karatzas, Ernest Valveny, and CV Jawahar.
 727 Infographicvqa. In *Proceedings of the IEEE/CVF Winter Conference on Applications of Computer
 728 Vision*, pp. 1697–1706, 2022.

729

730 Guofeng Mei, Wei Lin, Luigi Riz, Yujiao Wu, Fabio Poiesi, and Yiming Wang. Perla: Perceptive 3d
 731 language assistant. In *Proceedings of the Computer Vision and Pattern Recognition Conference*,
 732 pp. 14369–14379, 2025.

733

734 Nitesh Methani, Pritha Ganguly, Mitesh M Khapra, and Pratyush Kumar. Plotqa: Reasoning over
 735 scientific plots. In *Proceedings of the ieee/cvf winter conference on applications of computer
 736 vision*, pp. 1527–1536, 2020.

737

738 M Jehanzeb Mirza, Mengjie Zhao, Zhuoyuan Mao, Sivan Doveh, Wei Lin, Paul Gavrikov, Michael
 739 Dorkenwald, Shiqi Yang, Saurav Jha, Hiromi Wakaki, et al. GLOV: Guided Large Language
 740 Models as Implicit Optimizers for Vision Language Models. *arXiv preprint arXiv:2410.06154*,
 2025.

741

742 Mistral. Nemo. <https://mistral.ai/news/mistral-nemo/>, 2024. Large language
 743 model.

744

745 Atsuyuki Miyai, Jingkang Yang, Jingyang Zhang, Yifei Ming, Qing Yu, Go Irie, Yixuan Li, Hai Li,
 746 Ziwei Liu, and Kiyoharu Aizawa. Unsolvable problem detection: Evaluating trustworthiness of
 747 large multimodal models. 2024.

748

749 Linyong Nan, Chiachun Hsieh, Ziming Mao, Xi Victoria Lin, Neha Verma, Rui Zhang, Wojciech
 750 Kryściński, Hailey Schoelkopf, Riley Kong, Xiangru Tang, et al. Fetaqa: Free-form table question
 751 answering. *Transactions of the Association for Computational Linguistics*, 10:35–49, 2022.

752

753 OpenAI. Gpt-5. <https://chat.openai.com/>, 2025. Large language model.

754

755 Shraman Pramanick, Rama Chellappa, and Subhashini Venugopalan. Spiqa: A dataset for mul-
 756 timodal question answering on scientific papers. *Advances in Neural Information Processing
 757 Systems*, 37:118807–118833, 2024.

756 Abhilasha Ravichander, Eduard Hovy, Kaheer Suleman, Adam Trischler, and Jackie Chi Kit Che-
 757 ung. On the systematicity of probing contextualized word representations: The case of hypernymy
 758 in bert. In *Proceedings of the Ninth Joint Conference on Lexical and Computational Semantics*,
 759 pp. 88–102, 2020.

760 Jonathan Roberts, Kai Han, Neil Houlsby, and Samuel Albanie. Scifibench: Benchmarking large
 761 multimodal models for scientific figure interpretation. *Advances in Neural Information Processing
 762 Systems*, 37:18695–18728, 2024.

763 Rohit Saxena, Pasquale Minervini, and Frank Keller. Postersum: A multimodal benchmark for
 764 scientific poster summarization, 2025. URL <https://arxiv.org/abs/2502.17540>.

765 Nimrod Shabtay, Felipe Maia Polo, Sivan Doveh, Wei Lin, M. Jehanzeb Mirza, Leshem Chosen,
 766 Mikhail Yurochkin, Yuekai Sun, Assaf Arbelle, Leonid Karlinsky, and Raja Giryes. Livexiv –
 767 a multi-modal live benchmark based on arxiv papers content, 2025. URL <https://arxiv.org/abs/2410.10783>.

768 Baifeng Shi, Boyi Li, Han Cai, Yao Lu, Sifei Liu, Marco Pavone, Jan Kautz, Song Han, Trevor
 769 Darrell, Pavlo Molchanov, and Hongxu Yin. Scaling vision pre-training to 4k resolution, 2025.
 770 URL <https://arxiv.org/abs/2503.19903>.

771 Shruti Singh, Nandan Sarkar, and Arman Cohan. Scidqa: A deep reading comprehension dataset
 772 over scientific papers, 2024. URL <https://arxiv.org/abs/2411.05338>.

773 Zusheng Tan, Xinyi Zhong, Jing-Yu Ji, Wei Jiang, and Billy Chiu. Enhancing large language models
 774 for scientific multimodal summarization with multimodal output. In *Proceedings of the 31st
 775 International Conference on Computational Linguistics: Industry Track*, pp. 263–275, 2025.

776 Andreea-Maria Tanasă and Simona-Vasilica Oprea. Rethinking chart understanding using multi-
 777 modal large language models. *Computers, Materials & Continua*, 84(2), 2025.

778 Gemma Team, Morgane Riviere, Shreya Pathak, Pier Giuseppe Sessa, Cassidy Hardin, Surya Bhu-
 779 patiraju, Léonard Hussenot, Thomas Mesnard, Bobak Shahriari, Alexandre Ramé, et al. Gemma
 780 2: Improving open language models at a practical size. 2024. URL <https://arxiv.org/abs/2408.00118>.

781 Gemma Team, Aishwarya Kamath, Johan Ferret, Shreya Pathak, Nino Vieillard, Ramona Merhej,
 782 Sarah Perrin, Tatiana Matejovicova, Alexandre Ramé, Morgane Rivière, et al. Gemma 3 technical
 783 report. 2025. URL <https://arxiv.org/abs/2503.19786>.

784 Alex Turner and Mark Kurzeja. Gaming truthfulqa: Simple heuristics exposed dataset weaknesses,
 785 2025.

786 Adaku Uchendu, Thai Le, and Dongwon Lee. Attribution and obfuscation of neural text author-
 787 ship: A data mining perspective. *SIGKDD Explor. Newsl.*, 25(1):1–18, July 2023. ISSN 1931-
 788 0145. doi: 10.1145/3606274.3606276. URL <https://doi.org/10.1145/3606274.3606276>.

789 Alex Wang, Kyunghyun Cho, and Mike Lewis. Asking and answering questions to evaluate the
 790 factual consistency of summaries, 2020. URL <https://arxiv.org/abs/2004.04228>.

791 Yubo Wang, Xueguang Ma, Ge Zhang, Yuansheng Ni, Abhranil Chandra, Shiguang Guo, Weiming
 792 Ren, Aaran Arulraj, Xuan He, Ziyan Jiang, Tianle Li, Max Ku, Kai Wang, Alex Zhuang, Rongqi
 793 Fan, Xiang Yue, and Wenhui Chen. Mmlu-pro: A more robust and challenging multi-task language
 794 understanding benchmark, 2024a. URL <https://arxiv.org/abs/2406.01574>.

795 Yubo Wang, Xueguang Ma, Ge Zhang, Yuansheng Ni, Abhranil Chandra, Shiguang Guo, Weiming
 796 Ren, Aaran Arulraj, Xuan He, Ziyan Jiang, et al. Mmlu-pro: A more robust and challenging multi-
 797 task language understanding benchmark. *Advances in Neural Information Processing Systems*,
 798 37:95266–95290, 2024b.

799 Yifan Wu, Lutao Yan, Leixian Shen, Yunhai Wang, Nan Tang, and Yuyu Luo. Chartinsights: Eval-
 800 uating multimodal large language models for low-level chart question answering, 2024. URL
 801 <https://arxiv.org/abs/2405.07001>.

810 Qianqi Yan, Yue Fan, Hongquan Li, Shan Jiang, Yang Zhao, Xinze Guan, Ching-Chen Kuo, and
 811 Xin Eric Wang. Multimodal inconsistency reasoning (mmir): A new benchmark for multimodal
 812 reasoning models, 2025. URL <https://arxiv.org/abs/2502.16033>.

813

814 An Yang, Anfeng Li, Baosong Yang, Beichen Zhang, Binyuan Hui, Bo Zheng, Bowen Yu, Chang
 815 Gao, Chengen Huang, Chenxu Lv, et al. Qwen3 technical report. 2025a. URL <https://arxiv.org/abs/2505.09388>.

816

817 Haiqi Yang, Jinzhe Li, Gengxu Li, Yi Chang, and Yuan Wu. Can large multimodal models actively
 818 recognize faulty inputs? a systematic evaluation framework of their input scrutiny ability, 2025b.
 819 URL <https://arxiv.org/abs/2508.04017>.

820

821 Wenhui Yu, Gengshen Wu, and Jungong Han. Deep multimodal-interactive document summariza-
 822 tion network and its cross-modal text–image retrieval application for future smart city information
 823 management systems. *Smart Cities*, 8(3):96, 2025.

824

825 Rowan Zellers, Ari Holtzman, Yonatan Bisk, Ali Farhadi, and Yejin Choi. Hellaswag: Can a ma-
 chine really finish your sentence? 2019. URL <https://arxiv.org/abs/1905.07830>.

826

827 Pan Zhang, Xiaoyi Dong, Yuhang Zang, Yuhang Cao, Rui Qian, Lin Chen, Qipeng Guo, Haodong
 828 Duan, Bin Wang, Linke Ouyang, et al. Internlm-xcomposer-2.5: A versatile large vision lan-
 829 guage model supporting long-contextual input and output, 2024a. URL <https://arxiv.org/abs/2407.03320>.

830

831 Renrui Zhang, Dongzhi Jiang, Yichi Zhang, Haokun Lin, Ziyu Guo, Pengshuo Qiu, Aojun Zhou,
 832 Pan Lu, Kai-Wei Chang, Yu Qiao, et al. Mathverse: Does your multi-modal llm truly see the
 833 diagrams in visual math problems? In *European Conference on Computer Vision*, pp. 169–186.
 834 Springer, 2024b.

835

836 Yuhui Zhang, Yuchang Su, Yiming Liu, Xiaohan Wang, James Burgess, Elaine Sui, Chenyu Wang,
 837 Josiah Aklilu, Alejandro Lozano, Anjiang Wei, et al. Automated generation of challenging
 838 multiple-choice questions for vision language model evaluation. In *Proceedings of the Computer
 Vision and Pattern Recognition Conference*, pp. 29580–29590, 2025.

839

840 Fengbin Zhu, Wenqiang Lei, Fuli Feng, Chao Wang, Haozhou Zhang, and Tat-Seng Chua. To-
 841 wards complex document understanding by discrete reasoning. In *Proceedings of the 30th ACM
 842 International Conference on Multimedia*, pp. 4857–4866, 2022.

843

844 Jinguo Zhu, Weiyun Wang, Zhe Chen, Zhaoyang Liu, Shenglong Ye, Lixin Gu, Hao Tian, Yuchen
 845 Duan, Weijie Su, Jie Shao, et al. Internvl3: Exploring advanced training and test-time recipes for
 846 open-source multimodal models. 2025. URL <https://arxiv.org/abs/2504.10479>.

847

848

849

850

851

852

853

854

855

856

857

858

859

860

861

862

863

864 APPENDIX
865

866 In the appendix, we first discuss the **source code** (App. A) and **qualitative examples** (App. B),
 867 including a dataset viewer and examples of text-table and figure-equation inconsistencies. We then
 868 provide a comprehensive **list of assets** (App. C), detailing the data sources, licenses, and models
 869 used, including both open-source and proprietary ones. The **ablations section** (App. D) explores the
 870 impact of rasterization resolution on model performance and analyzes the effectiveness of Chain-of-
 871 Thought (CoT) reasoning with a detailed case study. The **dataset construction section** (App. E.1)
 872 explains our refined methodology for sourcing, filtering, and annotating inconsistencies from sci-
 873 entific papers, including a discussion of the annotation criteria, a custom-built annotation tool, and
 874 dataset statistics. Next, we detail the **process of generating LLM-based questions** (App. E.4) for
 875 our benchmark tasks (Inconsistency Identification, Remedy, and Pair-Match), including our debias-
 876 ing strategies using structured JSON representations. Finally, we provide details on the **user study**
 877 **implementation** (App. F), the **full LLM prompts** (App. G) used for various tasks, and **screenshots**
 878 (App. H and I) of our annotation and survey applications to provide a clear understanding of our
 879 methodology.

880 A SOURCE CODE
881

882 We provide the full source code for (1) the creation and evaluation of the benchmark dataset, (2)
 883 the annotation viewer and (3) the survey web app in the supplementary materials. More information
 884 on the structure and instructions on how to run the code is provided in a 'README.md' file in
 885 'source_code' folder of the material. Upon acceptance, we will release the source code publicly.
 886

887 B QUALITATIVE EXAMPLES AND DATASET VIEWER
888

889 Alongside the source code, the supplementary materials contain an annotation viewer, which can be
 890 used to visually explore our dataset in the web browser. The viewer can be launched by opening
 891 the `index.html` file inside the `annotation_viewer` folder (we recommend using Google
 892 Chrome).

893 We furthermore show qualitative examples of a text-table inconsistency (Fig. 3) and a figure-
 894 equation inconsistency (Fig. 4), together with their corresponding evaluation tasks.
 895

896 Again, the full dataset will be released publicly upon acceptance.
 897

898 C LIST OF ASSETS
899

900 Our images and annotations are sourced from publicly available datasets, and we distribute our data
 901 in compliance with the licensing terms of the original sources.
 902

903 The document and review data source can be found here:

- 904 • ICLR 2024 on OpenReview (<https://openreview.net/group?id=ICLR.cc/2024/Conference>):
 905 All papers were released under the CC BY 4.0 license. (before:)
- 906 • ICLR 2025 on OpenReview (<https://openreview.net/group?id=ICLR.cc/2025/Conference>):
 907 All papers were released under the CC BY 4.0 license.

908 The list of source code and model weights can be found here:

- 911 • Qwen2.5-VL (<https://github.com/QwenLM/Qwen2.5-VL>): Released under the Apache-2.0
 912 license.
- 913 • LLaVA-NeXT (<https://github.com/LLaVA-VL/LLaVA-NeXT>): Released under the
 914 Apache-2.0 license.
- 915 • Gemma 3 (<https://github.com/google-deepmind/gemma>): Released under the Apache-2.0
 916 license.
- 917 • Ovis 2 (<https://github.com/AIDC-AI/Ovis>): Released under the Apache-2.0 license.

918 • InternVL (<https://github.com/OpenGVLab/InternVL>): Released under the MIT license.
 919 • GLM-V (<https://github.com/zai-org/GLM-V>): Released under the Apache-2.0 license.
 920 • Mistral NeMo (<https://github.com/mistralai/mistral-inference>): Released under Apache-2.0
 921 license
 922 • vLLM (<https://github.com/vllm-project/vllm>): Released under the Apache-2.0 license.
 923 • MinerU (<https://github.com/opendatalab/MinerU>): Released under the AGPL-3.0 license.
 924

925 The list of proprietary models used can be found here:
 926

927 • Google Gemini (<https://deepmind.google/models/gemini/flash/>): Used in version Gemini
 928 Flash 2.5 and Gemini Pro 2.5, released on June 17, 2025.
 929 • OpenAI GPT (<https://github.com/LLaVA-VL/LLaVA-NeXT>): Used in version GPT-5, re-
 930 leased on August 7, 2025.
 931

932 D ABLATIONS

934 D.1 IMPACT OF RASTERIZATION RESOLUTION

936 Scientific papers contain dense text and fine-grained visual elements such as axis labels, annotations,
 937 and subscripts, which are often crucial for detecting subtle inconsistencies. To test whether rasteri-
 938 zation resolution impacts detection performance, we varied the DPI used to extract images from the
 939 PDF and evaluated a representative set of strongest proprietary and open-weight models of different
 940 sizes on the *Ident* task with *Focused Context*, keeping all other settings fixed.
 941

942 Table 4: Accuracy of LMMs under different rasterization resolutions. Results are reported for the
 943 *Ident* task with *Focused Context*. Percentage change is calculated relative to the 144 DPI baseline.
 944

DPI	VILA HD 4K 8B		InternVL3.5 8B		InternVL3.5 38B		Ovis2 34B		Gemini 2.5 Pro	
	Default	% Change	Default	% Change	Default	% Change	Default	% Change	Default	% Change
72	31.3	+1.3	42.7	-12.7	45.8	-20.1	43.1	-13.1	67.2	-3.3
144	30.9	-	48.9	-	57.3	-	49.6	-	69.5	-
300	29.4	-4.9	45.4	-7.2	51.9	-9.4	50.4	+1.6	70.6	+1.6

945 **Low resolutions harm performance.** Most models showed significant drops at 72 DPI, up to -
 946 20.1% for InternVL3.5 38B. Open-weight models were generally more vulnerable, though even
 947 Gemini 2.5 Pro declined by -3.3%. Surprisingly, VILA HD, despite being trained for high-resolution
 948 inputs, showed a slight accuracy gain at this lower setting.
 949

950 **Higher resolutions do not always improve accuracy.** Increasing from 144 to 300 DPI yielded
 951 mixed outcomes. While Gemini 2.5 Pro and Ovis2 34B benefited slightly, InternVL models per-
 952 formed worse, and VILA HD again failed to leverage the higher fidelity despite its specialized train-
 953 ing. This suggests that additional detail can sometimes overwhelm global reasoning or misalign
 954 with training distributions.
 955

956 **Resolution sensitivity is architecture-specific.** Overall, the assumption that higher resolution im-
 957 proves inconsistency detection does not hold universally. Performance varies with model design and
 958 pretraining data, and high-resolution training does not guarantee an edge in handling scientific in-
 959 consistencies. Careful DPI control is critical for fair evaluation. In our benchmark, 144 DPI provides
 960 a practical balance of visual clarity, computational cost, and cross-model comparability.
 961

962 D.2 CHAIN-OF-THOUGHT REASONING

963 Reasoning variants perform better than non-reasoning counterparts and reach results comparable to
 964 much larger models. For instance, InternVL3.5 8B achieves an average of **37.7%** (before: **37.6%**),
 965 rivaling large open-weight models and surpassing several 72B non-reasoning models. We therefore
 966 study how reasoning-enabled models leverage chain-of-thought (CoT) to improve performance on
 967 PRISMM-Bench. To do so, we re-evaluated a selection of reasoning models on the *Ident* task with
 968 *Focused Context* with reasoning turned off and compared the performance.
 969

972 Disabling reasoning reveals the critical role of CoT in detecting subtle inconsistencies. For example,
 973 GLM 4.5V drops from 51.8% to 43.2% (-16.6%) (before: 55.7% to 46.6% (-16.3%)), InternVL3.5
 974 8B from 49.5% to 40.6% (-18.0%) (before: 48.9% to 40.0% (-18.2%)), and InternVL3.5 38B suffers
 975 the largest decline, from 54.4% to 40.4% (-25.7%) (before: 57.4% to 37.8% (-34.0%)).
 976

977 **Why Reasoning Helps.** To understand these gains, we focused on inconsistencies where InternVL3.5 38B succeeded with reasoning but failed without. We identified three consistent patterns: (1) **Structured input handling.** Reasoning-enabled models interpret the JSON-formatted options in natural language, clarifying subtle distinctions without exploring linguistic biases (cf. low without-context performance for reasoning models in Sec. 4.3). (2) **Cross-modal grounding.** CoT traces show models explicitly reasoning over both text and visuals, breaking complex information into smaller units and reusing them later in the reasoning chain. (3) **Concept linking.** Reasoning enables models to connect fine-grained context with domain knowledge and abstract concepts, allowing stronger logical inference beyond surface pattern recognition.
 985

986 **Case Study.** Fig. 5 illustrates this effect with the *Unique Successful Jailbreaks* metric, which must
 987 be non-negative. The figure, however, contains error bars extending below zeros, resulting in an
 988 inconsistency.
 989

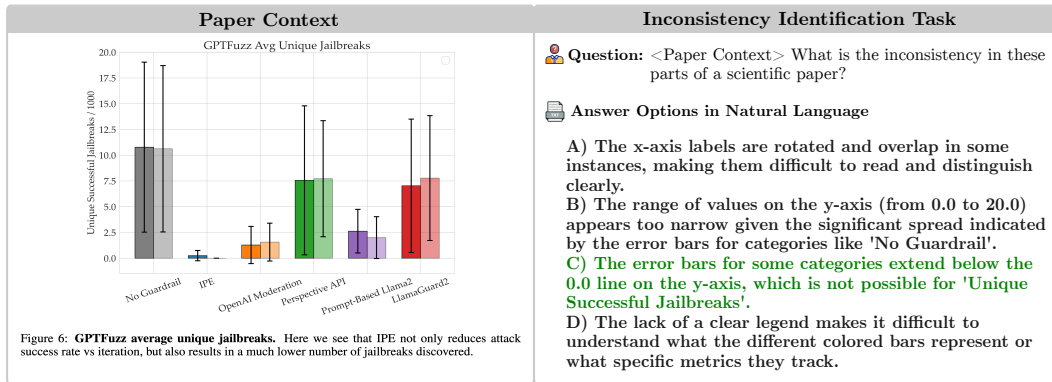


Figure 5: Inconsistency example for case study. Right: Visual context. Left: Question and answer options for *Ident* task. Natural language options used for ease-of-comprehension, LMM was tasked using JSON.

Without reasoning, InternVL3.5 38B selected the distractor “x-axis labels overlap,” (option A) justifying it with a generic but factually incorrect critique, as the labels were perfectly legible. The model defaulted to a template-like response rather than verifying claims against visual evidence.

In contrast, the reasoning-enabled model produced a systematic chain-of-thought: (1) ruling out label overlap (by observing the labels were ‘spaced out and readable’), (2) confirming the y-axis range was sufficient (noting all data was ‘within the 0-20 range’), (3) dismissing legend critiques (since a legend ‘isn’t necessary’ when bars are directly labeled), and (4) crucially, identifying the logical error of error bars that ‘shouldn’t go below zero if the metric [...] can’t be negative’). This stepwise elimination and domain-aware inference led to the correct answer. The full reasoning chain of InternVL3.5 38B is available in Fig. 6.

This case highlights two key strengths of reasoning: (1) systematic elimination of distractors, and (2) integration of domain knowledge (e.g. non-negativity of counts) with visual grounding. Although reasoning increase output length (average of 473 tokens per query in our case), it substantially improves multimodal consistency and robustness, making CoT a key mechanism for handling subtle scientific document inconsistencies.

1026 E DATASET CONSTRUCTION
10271028 E.1 REVIEW SOURCING
1029

1030 **Initial Exploration with Regex Matching.** Before finalizing the review sourcing strategy described
1031 in the main paper, we conducted an exploratory study to detect potential inconsistencies mentioned
1032 in reviews for ICLR 2024 using a simple regular expression (regex) approach. Reviews were ac-
1033 cessed via the OpenReview API², focusing on the “Weaknesses” and “Questions” sections, which
1034 were most likely to contain critical feedback. Each sentence was parsed for co-occurrence of terms
1035 related to inconsistencies (e.g., “mismatch”, “conflict”) and references to visual elements (e.g., “fig-
1036 ure”, “table”, “equation”). The pseudocode for this procedure is shown below:

1037
1038 **Algorithm 1** Pseudocode for regex matching

```

1: DEFINEPATTERN(inconsistency_pattern, r' (inconsisten | mismatch |
1039      doesn[']t match | not match |conflict | discrepanc)')
1040 2: DEFINEPATTERN(visual_pattern, r' (figure | fig.? | table | graph | plot
1041      | image | diagram | equation)')
1042
1043 3: results ← []
1044 4: for each review in reviews do
1045      sections ← EXTRACTSECTIONS(review)
1046      for each section in sections do
1047          sentences ← SPLITINTOSENTENCES(section)
1048          for each sentence in sentences do
1049              if MATCHES(sentence, inconsistency_pattern) and MATCHES(sentence, vi-
1050                  sual_pattern) then
1051                  APPEND(results, sentence)
1052              end if
1053          end for
1054      end for
1055 14: end for
1056 15: return results

```

1057 Manual inspection confirmed that reviews indeed contained valuable references to visual-textual
1058 mismatches. However, two limitations emerged: (1) regex captured only strict keyword formula-
1059 tions, missing paraphrased or indirect mentions of inconsistencies, and (2) many inconsistencies
1060 referenced papers that had been updated after rebuttal, making it impossible to locate the original
1061 errors in the PDF versions available through OpenReview.

1062 **Refined Collection Strategy.** To address these issues, we refined our strategy in two ways:

1063

1. **Conference selection:** We shifted our focus (before: to the more recent ICLR 2025, fo-
1064 cusing) on papers without author rebuttals. This ensured that flagged inconsistencies were
1065 more likely to remain in the available PDFs.
2. **LLM filtering:** Instead of regex, we employed *Mistral Nemo 2407* at a low temperature to
1066 summarize reviews and extract candidate inconsistency statements. This approach captured
1067 non-strict formulations (e.g., “does not align with” instead of “mismatch”) and produced
1068 structured outputs, making them easier to present to annotators in the verification interface.

1069 This refinement reduced our initial pool of 120,329 ICLR (before: 75,550 ICLR 2025) reviews to
1070 18,009 (before: 12,366) reviews. The LLM outputs were stored in structured JSON format, with
1071 each paper ID associated with a list of flagged inconsistencies.

1072 **Example Output.** Throughout the appendix, we are going to illustrate our data preparation pipeline
1073 use the paper ID vXSCD3ToCS³ as an example. We illustrate the example out after the LLM-
1074 assisted filtering in Fig. 7.

1075
1076
1077
1078
1079 ²<https://docs.openreview.net/reference/api-v2>

³<https://openreview.net/forum?id=vXSCD3ToCS>

1080 This structured representation provided a natural starting point for the subsequent manual verifica-
 1081 tion stage described in App. E.2.
 1082

1083 **E.2 ANNOTATION PROCESS**
 1084

1085 **Annotator Background.** The annotation was conducted by the first author, who has an advanced
 1086 background in Computer Science and Machine Learning. A consistent annotation standard was
 1087 maintained throughout the project; any ambiguous or borderline cases were discussed with senior
 1088 researchers until a consensus was reached.
 1089

1090 **Annotation Criteria.** During manual verification, the annotator judged each reviewer comment
 1091 against the following criteria:
 1092

- 1092 1. The comment reflects objective feedback rather than a subjective suggestion.
 1093
- 1093 2. The comment describes an inconsistency involving two contradicting facts.
 1094
- 1094 3. Both conflicting parts can be located in the PDF.
 1095
- 1095 4. The inconsistency can be identified without deep domain-specific expertise (focus on
 1096 visual/document-level inconsistencies).
 1097
- 1097 5. The inconsistency is significant and factual, not a minor typo or stylistic choice.
 1098

1100 **Annotation Interface.** We implemented a custom web-based tool in `Next.js`. The interface
 1101 displayed the reviewer’s comment (extracted by the LLM) alongside the corresponding paper em-
 1102 bedded as a PDF viewer (compare Fig. 18, Fig. 19 for screenshots of the app’s interface). The
 1103 annotator could:
 1104

- 1104 • Read the reviewer’s comment and decide whether it fulfilled criteria (1) and (2). If not, the
 1105 instance was skipped.
 1106
- 1106 • Search and inspect the relevant region of the embedded PDF.
 1107
- 1107 • Toggle between *one-part* and *two-part* annotation modes:
 - 1108 – **One-part:** A single element (e.g., figure-caption inconsistency).
 - 1109 – **Two-part:** Two separate elements (e.g., figure vs. text, or figure vs. figure).
- 1110 • Specify for each part whether it was textual or visual:
 - 1111 – *Visual:* Select the page, then draw a bounding box on a rendered thumbnail version
 the PDF page.
 - 1112 – *Textual:* Enter the page and line number, and copy the relevant text snippet from the
 PDF.
- 1113 • Assign an inconsistency category via a drop-down menu.
 1114
- 1114 • Provide a short free-text description of the inconsistency in their own words.
 1115

1116 **Recorded Metadata.** Each annotation combined automatically and manually collected fields:
 1117

- 1118 • **Automatically recorded:** element type (text or image), bounding box (relative coordi-
 1119 nates) for visual selections, internal image identifier, reviewer’s original comment.
 1120
- 1120 • **Manually entered:** page and line numbers, copied textual content, inconsistency category,
 1121 and a short description by the annotator.
 1122

1123 **Example Output.** Annotations were stored in JSON format, combining visual/textual parts, re-
 1124 viewer comment, category, and description. We illustrate the example annotation output in JSON
 1125 format in Fig. 8.
 1126

1127 **E.3 STATISTICS OF INCONSISTENCY COLLECTION.**
 1128

1129 The annotation resulted in 384 (before: 262) inconsistencies from 353 (before: 242) ICLR papers.
 1130 The average page count of each PDF was 16 (before: 18) pages. A total of 29 papers (7.6%)
 1131

1134 (before: 19 papers (7.9%)) had more than one inconsistency. The paper subjects were equally
 1135 distributed across the range of topics for ICLR (before: 2025)⁴, with (1) representation learning
 1136 (26.0%) (before: (14.5%)), (2) transfer learning (10.4%) (before: (11.2%)), (3) generative models
 1137 (9.6%) (before: datasets and benchmarks (10.8%)) and datasets and benchmarks (7.8%) (before:
 1138 (generative models 9.5%)) being the most frequent topics.

1139 We identified 15 (before: 13) categories of inconsistencies based on the elements involved, with the
 1140 distribution shown in Fig. 9. The most common cases were figure–text mismatches and intra-figure
 1141 inconsistencies.
 1142

1143 E.4 LLM-BASED QUESTION GENERATION

1144 E.4.1 INCONSISTENCY IDENTIFICATION (IDENT)

1145 The *Inconsistency Identification (Ident)* task was the first benchmark task we designed. For each
 1146 annotated inconsistency, we instructed *Gemini Flash* to generate a multiple-choice question (MCQ)
 1147 with four options, one of which correctly describes the inconsistency.
 1148

1149 **Inputs.** As input to the model, we provided:
 1150

- 1152 • The annotated context (visual and/or textual parts).
- 1153 • The annotator’s free-text description of the inconsistency.

1154 **Prompt.** After experimenting with several formulations, we found that a minimalist prompt yielded
 1155 the most creative and plausible distractors. We provide the final version of the prompt in Fig. 10.
 1156

1157 **Output Format.** The model produced a structured output containing the question, the correct an-
 1158 swer, and three distractor answers.
 1159

1160 **Manual Verification.** Each generated question underwent manual verification:
 1161

- 1162 • **Correct answer:** must (1) faithfully reflect the annotator’s description and (2) directly
 1163 connect to the annotated context.
- 1164 • **Distractors:** must (1) be grounded in the annotated inconsistency parts, (2) avoid obvious
 1165 contradictions within the answer itself, (3) only mention elements present in the provided
 1166 context, and (4) describe an inconsistency rather than confirming a correct fact from the
 1167 paper

1168 We also post-processed the text to remove stylistic artifacts often appended by the LLM, e.g. the
 1169 parenthetical “, *indicating an inconsistency*.”
 1170

1171 **Example Output.** We illustrate an example of the generated multiple-choice question for inconsis-
 1172 tency identification task in Fig. 11.
 1173

1174 E.4.2 DEBIASING THE INCONSISTENCY IDENTIFICATION TASK

1175 **Initial Observations.** When first evaluating the *Ident* task with *Gemini 2.5 Flash*, we observed
 1176 unexpectedly high accuracy:
 1177

- 1178 • 84.4% with the original LLM-generated questions. (e.g.: “*What inconsistency is observed
 1179 between Figure 2 and the accompanying text regarding the generated road network?*”)
- 1180 • 79.4% after replacing the LLM-generated question with the generic formulation: “*What is
 1181 the inconsistency in these parts of a scientific paper?*”

1182 Even in a sanity check where the model was shown only the question and answer options (without
 1183 the annotated context), performance remained at 57.6% accuracy, far above the random baseline of
 1184 25%. This indicated strong reliance on linguistic cues in the answer phrasing.
 1185

1186 ⁴<https://iclr.cc/Conferences/2025/CallForPapers>

1188 **Mitigation Strategies.** Moving forward, we solely employed the generic question formulation
 1189 throughout all inconsistencies. For reducing the without context accuracy Acc_{nc} , we systematically
 1190 explored ways of reducing linguistic priors by rewriting the answer options:
 1191

- 1192 • Normalizing answer length: $Acc_{nc} = 48.1\%$.
- 1193 • Filtering for MCQs where the correct answer is shortest: $Acc_{nc} = 46.2\%$.
- 1194 • Rephrasing distractors according to best practices in MCQ test design (Gierl et al., 2017):
 1195 $Acc_{nc} = 41.6\%$.
- 1196 • Shortening all answer options into nominal style: $Acc_{nc} = 38.2\%$.

1198 While these interventions reduced bias, they did not remove it completely.

1200 **Structured Representation: Evidence–Claim JSON.** As a more robust solution, we abandoned
 1201 free-form natural language and introduced a structured, human-readable JSON representation that
 1202 removes stylistic cues while preserving the semantic contradiction. The schema is:

```
1203 {
1204   "letter": "A" | "B" | "C" | "D",
1205   "attribute": str,
1206   "claim": {
1207     "source": "expectation" | str,
1208     "statement": str
1209   },
1210   "evidence": {
1211     "source": str,
1212     "statement": str
1213   }
1214 }
```

1215 **Patterns.** Two patterns of contradiction are covered:

- 1216 • **Claim vs. Evidence:** A claim from one paper element is contradicted by evidence from
 another.
- 1217 • **Expectation vs. Evidence:** A claim contradicts common expectations of scientific correct-
 ness. In this case, the claim’s source is always “expectation”

1222 We prompted *Gemini 2.5 Flash* to convert the natural language MCQs into this structured format.
 1223 The full prompt can be inspected in App. G.2. A 20% subset was manually validated for consistency.

1224 **Effect on Model Behavior.** This representation further reduced the no-context accuracy to 34.0%.
 1225 Given the full context, accuracy on the new JSON format decreased from 79.4% to 69.5%. How-
 1226 ever, the fraction of performance attributable to visual grounding (Eq. 1) increased from 51.4% to
 1227 53.8%. Thus, the structured format acts as a regularizer, forcing models to rely more strongly on the
 1228 provided paper context.

1229 **Example Output.** For the running example, we illustrate the example of debiased output in the
 1230 evidence-claim JSON format for the inconsistency identification task in Fig. 12.

1232 E.4.3 INCONSISTENCY REMEDY TASK

1234 **Task Design.** The *Inconsistency Remedy (Remedy)* task extends beyond identifying an inconsi-
 1235 stency to determining how it can be resolved. To avoid linguistic artifacts, we directly employed a
 1236 structured representation in JSON format. This representation adapts the Evidence–Claim schema
 1237 to a more action-oriented form, the **Target–Action JSON**:

```
1238 {
1239   "letter": "A" | "B" | "C" | "D",
1240   "attribute": str,
1241   "target": str,
```

```

1242     "other_involved": str,
1243     "action": "modify" | "remove" | "add" | "reposition" | "replace",
1244     "edit_statement": str,
1245     "reason": str
1246   }
1247

```

1248 Here, attribute captures the element at issue, target specifies where the change is applied,
 1249 other_involved records additional parts if necessary, and the fields action, edit_statement, and reason
 1250 summarize the correction.

1251 **LLM Conversion Process.** We found that prompting an LLM to directly convert the natural lan-
 1252 guage MCQs from the *Ident* task into Target–Action JSON yielded the most reliable results in terms
 1253 of readability and correctness. The prompt is depicted in Sec. G.3.

1254 **Example Output.** Four our example used throughout this appendix, the task looks as follows: We
 1255 illustrate the example output in Target–Action JSON format for the inconsistency remedy task in
 1256 Fig. 13.

1258 E.4.4 INCONSISTENCY PAIR-MATCH TASK

1260 **Task Design.** The *Inconsistency Pair-Match (Match)* task focuses on the subset of inconsistencies
 1261 that involve two distinct visual parts. The model is presented with one element (text or visual) as
 1262 the question context and must identify the corresponding inconsistent visual element among four
 1263 options.

1264 **Filtering of Eligible Cases.** Not all inconsistency categories are suitable for pair matching. Cat-
 1265 egories where the contradiction is contained entirely within a single element (i.e., *figure-caption*,
 1266 *figure-only*, *table-only*, *table-caption*, *algorithm-only*) were excluded. This filtering left 135 out of
 1267 the 262 inconsistencies in the dataset.

1269 **Distractor Construction.** To ensure challenging and fair distractors, we extracted all figures, tables,
 1270 and equations from the 242 papers in our dataset using *MinerU*⁵, which produced image crops with
 1271 unique IDs, modality labels, and page numbers. We then implemented a python script to sample
 1272 distractors as follows:

- 1273 • Distractors were restricted to the same modality as the correct answer.
- 1274 • Preference was given to elements appearing on the same page or on adjacent pages to the
- 1275 correct element, so that distractors were topically similar.
- 1276 • Sampling was done within the same paper. Each paper contained enough visual elements
- 1277 of the same modality so we didn't have to fallback to using elements from other papers.

1279 This procedure reduced trivial elimination strategies (e.g., selecting “the only figure among tables”) and forced models to consider fine-grained inconsistencies.

1282 **Example Output.** In the running example, the annotated inconsistency links an in-line text with a
 1283 figure. The text is fixed as the question context, and the answer options are image IDs referring to
 1284 extracted figures, with one image ID being the correct image cropped in the annotations. We show
 1285 the example of output used in the inconsistency pair-match task in Fig. 14.

1286

1287 F USER STUDY IMPLEMENTATION & STATISTICS

1288

1289 **Setup.** We conducted the user study in online form, using a custom web app. The participants were
 1290 greeted with an onboarding screen, where they entered the following information to assess their
 1291 eligibility to be included in the user study: (1) email address, (2) academic field, (3) academic level
 1292 and(4) AI exposure. Afterwards, they were shown instructions for the survey and an introduction
 1293 into the question formats and different context modalities. For each participants, ten tasks were
 1294 randomly sampled from our dataset. For the first five tasks, the participants were shown the *Focused*

1295 ⁵<https://github.com/opendatalab/MinerU>

1296 *Context* with the exact cropped images and/or text passages from the paper. For the last five tasks,
 1297 the participants were instructed to open a link to the original PDF and use the whole document to
 1298 answer the question. In this case, they were provided with the visual element they should focus on
 1299 in the paper. Screenshots of the user interface are provided in appendix I.

1300 Upon submission, the following datapoints were saved automatically: (1) The task ID, (2) The
 1301 chosen answer by the participants, (3) whether the task was correctly answered with/without context,
 1302 (4) whether the question was accompanied by *Focused Context* or *Full Document Context* and (5)
 1303 the time it took the participants to answer each question.

1304 **Statistics.** Our eight participants all have a background in either artificial intelligence, computer sci-
 1305 ence or mathematics at an academic level of PhD or higher (7 PhD, 1 postdoc). All stated to exhibit
 1306 advanced exposure levels to AI, which we defined as being comfortable with reading, interpreting
 1307 and critically evaluating AI scientific literature. The median answer time for questions without pro-
 1308 vided visual context was 45s, with *Focused Context* 145s and with *Whole Document Context* 169s.
 1309 In 65% of the cases, participants changed their answers once provided with the context. In total,
 1310 participants processed 80 inconsistencies.

1312 G LLM PROMPTS

1313 Here we provide the full prompts used to instruct the LLMs.

1317 G.1 LLM PROMPT FOR REVIEW FILTERING

1318 We provide the prompt for LLM-based review filtering in Fig. 15. Given the reviewer’s comment, the
 1319 model is instructed in a chain-of-thought prompting manner to systematically analyze each desired
 1320 characteristic of a visual inconsistency. Few-shot examples help clarify the output format.

1322 G.2 LLM PROMPT FOR CONVERTING INTO EVIDENCE-CLAIM FORMAT

1324 We provide the prompt for LLM-assisted conversion of natural language answers (for the inconsis-
 1325 tency identification task) into evidence-claim JSON format in Fig. 16. The evidence-claim JSON
 1326 format is used as answer options in the inconsistency identification task. The structured JSON-based
 1327 answer representation is for mitigating the language biases in multiple-choice evaluation.

1329 G.3 LLM PROMPT FOR CONVERTING INTO TARGET-ACTION FORMAT

1331 We provide the prompt for LLM-assisted conversion of natural language answers (for the inconsis-
 1332 tency identification task) into target-action JSON format in Fig. 17. Based on the question-answer
 1333 pairs in inconsistency identification task, we generate question with answers for the inconsistency
 1334 remedy task. The target-action JSON format is used as answer options in the inconsistency remedy
 1335 task.

1336 H SCREENSHOTS OF THE ANNOTATION APP

1339 We show some examples of the interface of the annotation tool in Fig. 18 and Fig. 19.

1341 I SCREENSHOTS OF THE SURVEY APP

1343 We show some examples of the interface of the survey web interface in Fig. 20, Fig. 21 and Fig. 22.

1350

1351

1352

1353

1354

1355

1356

1357

1358

1359

1360

1361

1362

1363

1364

1365

1366

1367

1368

1369

1370

1371

1372

1373

1374

1375

1376

1377

1378

1379

1380

1381

1382

1383

1384

1385

1386

1387

1388

1389

1390

1391

1392

1393

1394

1395

1396

1397

1398

1399

1400

1401

1402

1403

Paper Context

Visual element:

Table 10: Hyperparameters

Parameter	Stocks	ETTh	MuJoCo	Energy	fMRI
Attention heads	4	4	4	4	4
Attention head dimension	16	16	16	24	24
Encoder layers	2	3	3	4	4
Decoder layers	2	2	2	3	4
Batch size	64	128	128	64	64
Alpha, α	1.0	0.1	0.1	0.5	0.1
Timesteps / Sampling steps	500	500	1000	1000	1000
Pre-trained training steps	10000	18000	14000	25000	25000

Textual element:

“ where η is a hyperparameter controlling the strength of the gradient guidance, γ balances the trade-off between fitting the observed data and adhering to the learned data distribution”

Inconsistency Identification Task

Question: <Paper Context> What is the inconsistency in these parts of a scientific paper?

Answer Options in JSON Format

```

A) {
  "letter": "A",
  "attribute": "eta and gamma hyperparameters",
  "claim": {
    "source": "text",
    "statement": "present"
  },
  "evidence": {
    "source": "Table 10",
    "statement": "missing"
  }
}

B) {
  "letter": "B",
  "attribute": "Attention heads",
  "claim": {
    "source": "expectation",
    "statement": "should be explained"
  },
  "evidence": {
    "source": "text",
    "statement": "not explained"
  }
}

```

Interpretation Aid - Read answer A as:
There is a **claim** made in the text about the **attribute** "eta and gamma hyperparameters" and that **claim** is that they are "present", but there is **evidence** in *Table 10* that they are "missing".

Inconsistency Remedy Task

Question: <Paper Context> What action needs to be taken to resolve the inconsistency in these parts of a scientific paper?

Answer Options in JSON Format

```

A) {
  "letter": "A",
  "attribute": "hyperparameters eta ( $\eta$ ) and gamma ( $\gamma$ )",
  "target": "table_10",
  "other_involved": "text",
  "action": "add",
  "edit_statement": "parameters",
  "reason": "missing"
}

B) {
  "letter": "B",
  "attribute": "attention heads",
  "target": "text",
  "other_involved": "table_10",
  "action": "add",
  "edit_statement": "explain",
  "reason": "missing"
}

```

Interpretation Aid - Read answer A as:
The **attribute** "hyperparameters eta (η) and gamma (γ)" in *Table 10* needs to be edited by **action** "add parameters" with the **reason** that they are "missing" compared to the other involved element "Text".

Inconsistency Pair-Match Task

Question: You are provided with a part of a scientific paper:
“ where η is a hyperparameter controlling the strength of the gradient guidance, γ balances the trade-off between fitting the observed data and adhering to the learned data distribution”
The combination with one of the other parts within the same paper results in an inconsistency. Pick the letter of the correct answer option.

Answer Options:

A)

Table 10: Hyperparameters

Parameter	Stocks	ETTh	MuJoCo	Energy	fMRI
Attention heads	4	4	4	4	4
Attention head dimension	16	16	16	24	24
Encoder layers	2	3	3	4	4
Decoder layers	2	2	2	3	4
Batch size	64	128	128	64	64
Alpha, α	1.0	0.1	0.1	0.5	0.1
Timesteps / Sampling steps	500	500	1000	1000	1000
Pre-trained training steps	10000	18000	14000	25000	25000

C)

Table 9: Statistics of datasets.

Dataset	#Rows	#Features	Source
Stocks	3773	6	https://finance.yahoo.com/quote/GOOG
ETTh	17420	7	https://github.com/zhouhaoyi/ETThdataset
MuJoCo	1049	14	https://github.com/deepmind/dm_control
Energy	19711	28	https://www.cs.toronto.edu/~davidm/datasets
fMRI	10000	50	https://www.fmribox.ac.uk/datasets

B)

Table 8: Results of four aggregation strategies on Stocks and fMRI datasets. **Bold** indicates best performance.

Metric	Setting	Stocks	fMRI
Crossval-FID	1, 1, 1, 1	0.993 ± 0.001	2.076 ± 0.001
	1, 1, 1, 1 (ours)	0.975 ± 0.001	1.459 ± 0.001
	1, 1, 1, 1 (ours)	0.975 ± 0.001	1.459 ± 0.001
Crossval	1, 1, 1, 1	0.988 ± 0.001	2.061 ± 0.001
	1, 1, 1, 1 (ours)	0.988 ± 0.001	2.061 ± 0.001
	1, 1, 1, 1 (ours)	0.988 ± 0.001	2.061 ± 0.001
Deterministic	1, 1, 1, 1	0.848 ± 0.001	0.426 ± 0.001
	1, 1, 1, 1 (ours)	0.845 ± 0.001	0.414 ± 0.001
	1, 1, 1, 1 (ours)	0.845 ± 0.001	0.414 ± 0.001
Predictive	1, 1, 1, 1	0.801 ± 0.001	0.335 ± 0.001
	1, 1, 1, 1 (ours)	0.801 ± 0.001	0.335 ± 0.001
	1, 1, 1, 1 (ours)	0.801 ± 0.001	0.335 ± 0.001

D)

Table 7: Results on multiple imbalanced partitioned datasets. **Bold** indicates best performance.

Metric	Method	Stocks	ETTh	MuJoCo	Energy	fMRI
Crossval-FID	Controlled*	1.912 ± 0.018	1.736 ± 0.020	1.933 ± 0.018	3.862 ± 0.020	1.211 ± 0.018
	Controlled	1.912 ± 0.018	1.736 ± 0.020	1.933 ± 0.018	3.862 ± 0.020	1.211 ± 0.018
	Controlled	1.912 ± 0.018	1.736 ± 0.020	1.933 ± 0.018	3.862 ± 0.020	1.211 ± 0.018
Crossval	Local	1.355 ± 0.000	0.913 ± 0.000	0.793 ± 0.000	0.652 ± 0.000	0.767 ± 0.000
	Controlled	1.355 ± 0.000	0.913 ± 0.000	0.793 ± 0.000	0.652 ± 0.000	0.767 ± 0.000
	Controlled	1.355 ± 0.000	0.913 ± 0.000	0.793 ± 0.000	0.652 ± 0.000	0.767 ± 0.000
Deterministic	Local	0.162 ± 0.000	0.162 ± 0.000	0.129 ± 0.000	0.415 ± 0.000	0.451 ± 0.000
	Controlled	0.162 ± 0.000	0.162 ± 0.000	0.129 ± 0.000	0.415 ± 0.000	0.451 ± 0.000
	Controlled	0.162 ± 0.000	0.162 ± 0.000	0.129 ± 0.000	0.415 ± 0.000	0.451 ± 0.000
Predictive	Local	0.169 ± 0.000	0.220 ± 0.000	0.118 ± 0.000	0.362 ± 0.000	0.441 ± 0.000
	Controlled	0.169 ± 0.000	0.220 ± 0.000	0.118 ± 0.000	0.362 ± 0.000	0.441 ± 0.000
	Controlled	0.169 ± 0.000	0.220 ± 0.000	0.118 ± 0.000	0.362 ± 0.000	0.441 ± 0.000

Figure 3: A qualitative example of a text–table inconsistency and its corresponding evaluation tasks of *Ident*, *Remedy* and *Match*.

26



Figure 4: A qualitative example of a figure-equation inconsistency and its corresponding evaluation tasks of *Ident*, *Remedy* and *Match*.

1458

1459

1460

1461

1462

1463

Full Reasoning Chain of InternVL 3.5 on inconsistency 3MDmM0rMPQ

1464

Okay, let's take a look at this question. The user is asking about inconsistencies in parts of a scientific paper based on the provided figure. The options are A to D, each pointing out a different potential issue.

1465

1466

1467

1468

First, I need to check each option against the figure provided. Let's start with option A: x-axis labels overlapping. Looking at the x-axis in Figure 6, the labels are "No Guardrail," "IPE," "OpenAI Moderation," "Perspective API," "Prompt-Based Llama2," and "LlamaGuard2." They seem to be spaced out and readable. There's no overlap here; each label is clearly visible. So A isn't the right answer.

1469

1470

1471

Option B mentions the y-axis range being too narrow. The y-axis goes from 0 to 20.0, and the data points are all below 15, with error bars extending up to around 18. If the range was too narrow, the error bars might get cut off. But in the figure, the error bars are within the 0-20 range. The maximum error bar seems to reach just under 20, so the range is sufficient. B is not correct.

1472

1473

1474

1475

Option C states that error bars should be non-negative but extend below 0. Looking at the error bars, especially for "IPE" and "OpenAI Moderation," the error bars go below the 0 line. For example, the "No Guardrail" bar has an error bar that dips below 0 on the y-axis. Since error bars represent variability, they shouldn't go below zero if the metric (like jailbreaks) can't be negative. This seems like a valid inconsistency. So C is the answer.

1476

1477

1478

Option D claims the legend isn't clear. The figure's legend uses different colors for each method, but the legend itself isn't shown in the image. However, the user's question refers to the figure's elements. Without a legend in the figure, that's an issue. But looking at the figure, each bar is labeled directly with the method name, so a legend isn't necessary. Therefore, D is not the issue here.

1479

1480

So, the most likely answer is C, because error bars extending below zero when the metric can't be negative is an

1481

1482

Figure 6: Raw reasoning output by InternVL3.5 38B on 3MDmM0rMPQ.

1483

1484

1485

1486

1487

1488

1489

1490

1491

1492

1493

Example Output After the LLM-assisted Filtering

1494

```
{
  "vXSCD3ToCS": {
    "has_inconsistency": true,
    "inconsistencies": [

```

1495

"Table 6: The performance improvement from using 20 years of data (MAE of 20.24) compared to 1 year (MAE of 21.90) in the 3-day setting is marginal, contradicting the emphasis on the scale of DynST as a major contribution.",

1496

"Figure 2: The bottom left corner shows a road segment between two points that is not represented as an edge in the topology, which appears inconsistent with the actual road network.",

1497

"Figure 5: The description of the figure suggests changes in sensors deployment, not actual road network dynamics, which contradicts the paper's claim of considering dynamic road network topology."

1498

```
  ]
}
```

1499

```
}
```

1500

1501

1502

1503

1504

1505

1506

1507

1508

1509

1510

1511

Figure 7: Example output after the LLM-assisted filtering.

```

1512
1513
1514
1515
1516
1517
1518
1519
1520
1521
1522
1523
1524
1525
1526
1527
1528
1529
1530
1531
1532
1533
1534
1535
1536
1537
1538
1539
1540
1541
1542
1543
1544
1545
1546
1547
1548
1549
1550
1551
1552
1553
1554
1555
1556
1557
1558
1559
1560
1561
1562
1563
1564
1565

```

Example Annotation Output in JSON Format

```
{
  "inconsistency_parts": [
    {
      "type": "image",
      "page": 5,
      "image_id": "vXSCD3ToCS_5_a1e8a4c6",
      "bbox": { "x": 0.5, "y": 0.25, "width": 0.35, "height": 0.31 }
    },
    {
      "type": "text",
      "page": 5,
      "line": 262,
      "content": "The results demonstrate ..."
    }
  ],
  "review_text": "Figure 2: The bottom left corner shows ...",
  "category": "figure-text",
  "description": "Missing edges between nodes compared to the claim."
}
```

Figure 8: Example annotation output in JSON format.

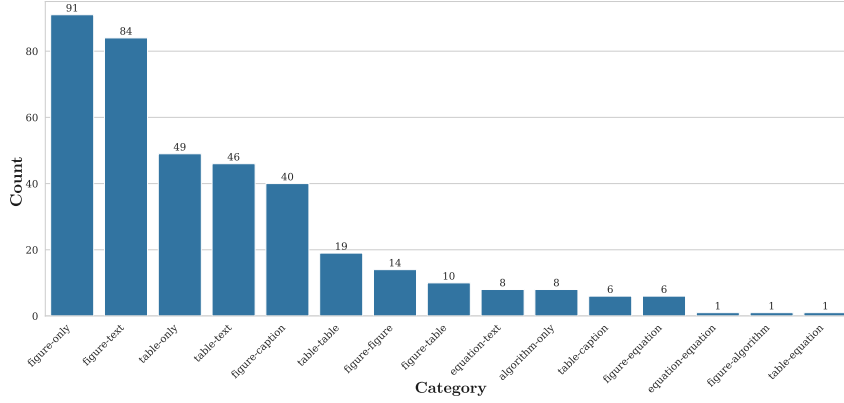


Figure 9: Distribution of inconsistency types. We identified 15 (before: 13) categories of inconsistencies based on the elements involved. The most common cases are figure-text mismatches and intra-figure (*figure-only*) inconsistencies **This figure has been updated to include statistics of the 122 new data points from ICLR 2024**

Prompt for Preparing MCQs in Inconsistency Identification Task

You are a visual assistant that can analyze image and text excerpts from scientific papers. You receive either one image, two images, or a pair of image and text that contain a visual inconsistency flagged by reviewers. Alongside the content, you also receive a description of the inconsistency. Based on these, generate a multiple-choice question testing the model's ability to detect the inconsistency. Follow these strict rules:

- The question should directly reference the provided content of the paper.
- There must be exactly 4 answer choices.
- Only one answer should correctly describe the inconsistency.
- The 3 distractors must be plausible but incorrect. They should either be incorrect due to omission or subtle misinterpretations of the content.
- Do not invent details beyond what is provided.
- Clearly label the correct answer.

Figure 10: Prompt for preparing multiple-choice questions in the inconsistency identification task.

1566

1567

1568

1569

1570

1571

1572

1573

1574

1575

1576

1577

1578

1579

1580

1581

1582

1583

1584

1585

1586

1587

Example of Generated MCQ in Inconsistency Identification Task

```
{
  "mcq": {
    "default": {
      "question": "What inconsistency is observed between Figure 2 and the accompanying text regarding the generated road network?",
      "correct": "The visualization in Figure 2 shows missing edges between nodes, which contradicts the text's claim that the generated network perfectly matches the actual road network structure.",
      "incorrect": [
        "The visualization in Figure 2 shows extraneous edges between nodes, which contradicts the text's claim that the generated network perfectly matches the actual road network structure.",
        "Figure 2 depicts only a disconnected portion of the road network, implying the algorithm did not generate the complete structure.",
        "The blue nodes in Figure 2 are unevenly distributed, making it difficult to determine the precise road paths."
      ],
      "letters": [
        "D", "A", "B", "C"
      ]
    }
  }
}
```

1588

1589

1590

Figure 11: Example of generated multiple-choice question for the inconsistency identification task.

1591

1592

1593

1594

1595

1596

1597

1598

1599

1600

1601

1602

1603

1604

1605

1606

1607

1608

1609

1610

1611

1612

1613

1614

1615

1616

1617

1618

1619

Example of Debiased Output in Evidence-Claim JSON Format

```
{
  "mcq": {
    "default": {
      "question": "What is the inconsistency in these parts of a scientific paper?",

      "correct": {
        "letter": "A",
        "attribute": "edges",
        "claim": {
          "source": "text",
          "statement": "perfectly matches"
        },
        "evidence": {
          "source": "Figure 2",
          "statement": "missing edges"
        }
      },

      "incorrect": [
        {
          "letter": "C",
          "attribute": "edges",
          "claim": {
            "source": "text",
            "statement": "perfectly matches"
          },
          "evidence": {
            "source": "Figure 2",
            "statement": "extraneous edges"
          }
        }
      ],
      "letters": [
        "A", "C", "D", "B"
      ]
    }
  }
}
```

Figure 12: Example of debiased output in evidence-claim JSON format for the inconsistency identification task.

1620

1621

1622

1623

```

1624     {
1625         "mcq": {
1626             "edit": {
1627                 "question": "What action needs to be
1628                 taken to resolve the inconsistency in these parts
1629                 of a scientific paper?",
1630                 "correct": {
1631                     "letter": "A",
1632                     "attribute": "edges",
1633                     "target": "figure_2",
1634                     "other_involved": "text",
1635                     "action": "add",
1636                     "edit_statement": "missing edges",
1637                     "reason": "contradicts claim"
1638                 },
1639                 "incorrect": [
1640                     {
1641                         "letter": "C",
1642                         "attribute": "edges",
1643                         "target": "figure_2",
1644                         "other_involved": "text",
1645                         "action": "remove",
1646                         "edit_statement": "extraneous edges",
1647                         "reason": "contradicts claim"
1648                     },
1649                     {
1650                         "letter": "D",
1651                         "attribute": "road network",
1652                         "target": "figure_2",
1653                         "other_involved": "algorithm",
1654                         "action": "modify",
1655                         "edit_statement": "disconnected portion",
1656                         "reason": "incomplete structure"
1657                     },
1658                     {
1659                         "letter": "B",
1660                         "attribute": "blue nodes",
1661                         "target": "figure_2",
1662                         "other_involved": null,
1663                         "action": "modify",
1664                         "edit_statement": "distribute nodes evenly",
1665                         "reason": "unclear paths"
1666                     }
1667                 ],
1668                 "letters": [
1669                     "A", "C", "D", "B"
1670                 ]
1671             }
1672         }
1673     }

```

Figure 13: Example of output in target-action JSON format for the inconsistency remedy task, directly converted from the natural language MCQs from the inconsistency identification task.

1649

1650

1651

1652

1653

1654

1655

1656

```

1657     {
1658         "mcq": {
1659             "part_pair": {
1660                 "question": "The results demonstrate that the adjacency matrix generated by our algorithm
1661                 perfectly matches the actual road network structure.",
1662                 "correct": "vXSCD3ToCS_5_ale8a4c6",
1663                 "incorrect": [
1664                     "vXSCD3ToCS_5_image_figure3",
1665                     "vXSCD3ToCS_5_image_figure4",
1666                     "vXSCD3ToCS_6_image_figure5"
1667                 ],
1668                 "letters": [
1669                     "D", "A", "C", "B"
1670                 ]
1671             }
1672         }
1673     }

```

Figure 14: Example output for the inconsistency pair-match task.

1674

1675 **Prompt for LLM-based Review Filtering**

1676 You are an AI assistant specialized in analyzing academic paper reviews. Your task is to identify inconsistencies

1677 between visual elements (such as figures and tables) and their corresponding text descriptions in the original paper

1678 being reviewed. These inconsistencies should be explicitly mentioned or highlighted by the reviewer in their review.

1679 Here is the paper review you need to analyze:

1680 <review>

1681 {prompt}

1682 </review>

1683 Instructions:

1684 1. Carefully read through the entire review.

1685 2. Focus exclusively on identifying instances where the reviewer mentions inconsistencies in the original paper

1686 between visual elements (figures, tables, graphs, etc.) and their corresponding text descriptions.

1687 3. For each identified inconsistency:

1688 a. Determine the type of mismatch (e.g., figure legend vs. content, text results vs. figure data, table values vs.

1689 text mentions)

1690 b. Note the specific location or reference in the original paper (e.g., figure number, table number, page number

1691 if available)

1692 c. Briefly describe the nature of the inconsistency as mentioned by the reviewer

1693 4. Disregard any general inconsistencies that are not related to vision-text mismatches in the original paper.

1694 Before providing your final response, analyze the review in <review_analysis> tags:

1695 5. List all mentions of visual elements in the review.

1696 6. For each visual element, note whether the reviewer mentions any inconsistencies with the text.

1697 7. For identified inconsistencies, write down the specific quote from the review that mentions it.

1698 This analysis will help ensure a thorough examination of the review and prevent misinterpretation of

1699 inconsistencies within the review itself versus those in the original paper.

1700 After your analysis, present your findings in JSON format. Each identified inconsistency should be an object in an

1701 array, with the following structure:

1702

```

1703 {
1704     "has_inconsistency": boolean,
1705     "inconsistencies": [
1706         "string (brief explanation of the inconsistency, always including the place in the original paper where it is
1707         located and as close to the reviewer's text as possible)", // Additional inconsistencies...
1708     ]
1709 }
1710
1711 }
```

1712 If no vision-text inconsistencies in the original paper are mentioned by the reviewer,

1713 return:

```

1714 {
1715     "has_inconsistency": false,
1716     "inconsistencies": []
1717 }
```

1718 Example of desired output structure (purely for format, not content):

```

1719 {
1720     "has_inconsistency": true,
1721     "inconsistencies": [
1722         "Table 1: The performance for model A is 69.74 percent but the text mentions 65.47 percent.",
1723         "The text refers to Group 1 and Group 0, but Figure 1 labels the groups as Group 1 and Group 2."
1724     ]
1725 }
```

1726 Remember to focus solely on vision-text mismatches in the original paper as mentioned by the reviewer. Provide

1727 clear, concise descriptions that make it easy for researchers to locate and verify the inconsistencies in the original

1728 paper based on the review's comments.

1729

Figure 15: Prompt for LLM-based review filtering.

1782
 1783
 1784
 1785
 1786
 1787
 1788
 1789
 1790 **Prompt for Converting Natural Language Answer into Target-Action JSON Format**
 1791
 1792 You are a system that converts multiple choice question answers about inconsistencies in scientific
 1793 papers into Target-Action JSON format. The goal is to identify what needs to be changed in the
 1794 paper to resolve the inconsistency.
 1795 Target-Action JSON format:
 1796 ```json
 1797 {
 1798 "letter": "A" | "B" | "C" | "D",
 1799 "attribute": str, // the core element at issue (e.g., legend, methods evaluated, F1 scores)
 1800 "target": str, // where the edit is applied (e.g., caption, figure_4b, table_5, equation_2)
 1801 "other_involved": str // (optional) other elements involved in the inconsistency, comma-separated
 1802 "action": "modify" | "remove" | "add" | "reposition" | "replace",
 1803 "edit_statement": str, // short 2-3 words description of the needed change (exclude word from
 1804 action)
 1805 "reason": str // why the change is needed in 2-3 words
 1806 }
 1807 ```
 1808 Example:
 1809 ```json
 1810 {
 1811 "letter": "C",
 1812 "attribute": "windows",
 1813 "target": "figure_1b",
 1814 "other_involved": "figure_1a",
 1815 "action": "modify",
 1816 "edit_statement": "align door position",
 1817 "reason": "different"
 1818 }
 1819 ```
 1820 Given:
 1821 - The question
 1822 - The answer options with letters (A, B, C, D)
 1823 - The correct answer letter
 1824 - The visual elements relevant to the inconsistency
 1825
 1826 Figure 17: Prompt for LLM-assisted conversion of natural language answers of the inconsistency
 1827 identification task into target-action JSON format. The target-action JSON is used as answer options
 1828 in the inconsistency remedy task.
 1829
 1830
 1831
 1832
 1833
 1834
 1835

1836

1837

1838

1839

1840

1841

1842

1843

1844

1845

1846

1847

1848

1849

1850

1851

1852

1853

1854

1855

1856

1857

1858

1859

1860

1861

1862

1863

1864

1865

1866

1867

1868

1869

1870

1871

1872

1873

1874

1875

1876

1877

1878

1879

1880

1881

1882

1883

1884

1885

1886

1887

1888

1889

Paper Inconsistency Annotation

 Export Batch (1)
 Export All

Completed	Valid Inconsistencies	Skipped
1/3 (33.3%)	0/1 (0.0%)	1/1 (100.0%)

[Skip This Inconsistency](#)

Progress

33.3% complete

2 of 3

 **Current Inconsistency**

Paper ID: vXSCD3ToCS

Figure 2: The bottom left corner shows a road segment between two points that is not represented as an edge in the topology, which appears inconsistent with the actual road network.

PDF Document

Under review as a conference paper at ICLR 2025

000 DYNST: L RGE-SC LE SP TI L-Tempor LD T SET
001 FOR TR NSFER BLE TR FFIC FOREC STING WITH DY-
002 N MIC RO D NETWORKS
003
004 anonymous authors
005 Paper under double-blind review
006
007
008
009
010
011
012
013
014
015
016
017
018
019
020
021
022
023
024
025
026
027
028
029
030
031
032
033
034
035
036
037
038
039
040
041
042
043
044
045
046
047
048
049
050
051
052
053

BSTR CT

In real-world traffic networks, it is common to encounter a shortage of historical data in the target region. Researchers often address this issue through transfer learning. However, transfer learning tasks in traffic prediction currently lack dedicated datasets and are based on datasets designed for non-transfer prediction tasks. The major drawback of these existing datasets is the adoption of a fixed network topology to model the world's road networks. This does not align with reality and limits a model's transferability. To tackle this issue, we propose DynST, a dataset specifically designed for transfer learning tasks in traffic prediction, with a massive data volume of 20.35 billion, spanning 20 years and 9 regions. The key feature of DynST is evolving dynamic road network topology, which reflects the evolution of real-world networks. Moreover, to address the shortcoming of the distance-based adjacency generation algorithm, we introduce a novel tree-based algorithm. Extensive experiments demonstrate that the adoption of DynST as the source dataset can significantly improve the traffic prediction in the target region. The comparative experiment also validates that our adjacency matrix generation algorithm can lead to improved prediction accuracy. We believe that DynST, with rich spatial variation information, will facilitate research in the field of transfer traffic prediction.

1 INTRODUCTION

Traffic forecasting plays a crucial role in urban management and travel planning, and relies heavily on historical data. In reality, the available data in the target areas are often inadequate, feasible approach is to utilize the transfer learning technique, where learnable knowledge learned from the source region is transferred to the target area through non-transfer learning tasks have been developed (Wang et al., 2021; Yin et al., 2022; Jin et al., 2022; Yao et al., 2019; Jin et al., 2022), there is currently no dataset specifically designed for the transfer learning task. These models typically leverage dataset properties of non-transfer learning, which primarily consists of an unlabeled dataset to generate knowledge for the target region (Yin et al., 2018; Li et al., 2017; Cui et al., 2019; Guo et al., 2020; Song et al., 2020; Liu et al., 2023b).

The existing datasets inherently assume the completeness of data and the invariance of the road network. In the real world, due to factors like weather conditions and equipment failure, data integrity is often violated in large-scale datasets (Wu et al., 2024). Additionally, it is meant for small road connections to evolve the road network topology (Chen et al., 2008). On the other hand, the nature of transfer learning tasks requires knowledge to be transferred between two regions with completely different topologies, but the same network topology. Intuitively, increasing the dynamics of the original region to be more unpredictable can help the target region. By exposing the model to a more diverse topology of road networks, it can learn more robust patterns that are less tied to specific nodes' characteristics. In contrast, a fixed road network topology in the source region may limit the model's transferability to adapt to new network structures.

Motivated by this, we propose DynST, a large-scale spatial-temporal dataset featuring evolving dynamic topology with data spanning up to 20 years, specifically designed for transfer learning tasks in traffic forecasting. The basic information is compared in Table 1. To construct DynST, we sourced

Enable second inconsistency part

Figure 18: First part of annotation app showing an overview over the annotation progress and embedded original PDF file.

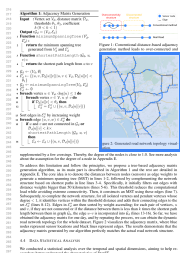
1890
 1891
 1892
 1893
 1894
 1895
 1896
 1897
 1898
 1899
 1900
 1901
 1902
 1903
 1904
 1905
 1906
 1907
 1908
 1909
 1910
 1911
 1912
 1913
 1914
 1915
 1916
 1917
 1918
 1919
 1920
 1921
 1922
 1923
 1924
 1925
 1926
 1927
 1928
 1929
 1930
 1931
 1932
 1933
 1934
 1935
 1936
 1937
 1938
 1939
 1940
 1941
 1942
 1943

First Inconsistency Part

Image Inconsistency

Page Number

Click and drag to select the inconsistency area in the image



Crop Selection

Second Inconsistency Part

Text Inconsistency

Page Number

Text Content

The results demonstrate that the adjacency matrix generated by our algorithm perfectly matches the actual road network structure.

Line Number

Annotation Metadata

Inconsistency Category

Description

We can see missing edges between nodes to perfectly match the road network structure as claimed in the text of the paper

Figure 19: Second part of annotation app for drawing bounding boxes, entering text and further details about the inconsistency.

1944
 1945
 1946
 1947
 1948
 1949
 1950
 1951
 1952
 1953
 1954
 1955
 1956
 1957
 1958
 1959
 1960
 1961
 1962
 1963
 1964
 1965
 1966
 1967
 1968
 1969
 1970
 1971
 1972
 1973
 1974
 1975
 1976
 1977
 1978
 1979
 1980
 1981
 1982
 1983
 1984
 1985
 1986
 1987
 1988
 1989
 1990
 1991
 1992
 1993
 1994
 1995
 1996
 1997

Research Survey
 Question 1 of 10 - Phase 1

Question (Phase 1: Initial Guess)

What is the inconsistency in these parts of a scientific paper?

The 'Original Question' uses a continuous 1-10 scale, but the 'Converted Statements' only group responses into four discrete ranges.

The 'Original Question' defines 1 as 'Completely Dissatisfied' and 10 as 'Completely Satisfied', whereas the 'Converted Statements' redefine the lower numbers (1,2) as 'very satisfied' and the higher numbers (9,10) as 'very dissatisfied'.

The 'Original Question' allows for open-ended 'Unstructured Survey Questions', while the 'Converted Statements' are limited to 253 pre-defined value-expressing statements, indicating a change in data type.

The inconsistency lies in the 'LMs' Predictions' section, where Person A and Person B exhibit different accuracy percentages (56% vs 67%).

Submit Initial Guess

Figure 20: First part of survey interface showing a question with no context provided.

1998
1999
2000
2001
2002
2003
2004
2005
2006
2007
2008
2009
2010
2011
2012
2013
2014
2015
2016
2017
2018
2019
2020
2021
2022
2023
2024
2025
2026
2027
2028
2029
2030
2031
2032
2033
2034
2035
2036
2037
2038
2039
2040
2041
2042
2043
2044
2045
2046
2047
2048
2049
2050
2051

Research Survey

Question 1 of 10 - Phase 2

Context

Original Question in World Value Survey (WVS)

Q10: All things considered, how satisfied are you with your life as a whole these days? Using this card on which 1 means you are "completely dissatisfied" and 10 means you are "completely satisfied" where would you put your satisfaction with your life as a whole?

Answer Options:
1 (Completely Dissatisfied)
10 (Completely Satisfied)

Converted Statements in INDIEVALUECATALOG

Unstructured Survey Questions

Evaluating LMs on Individualistic Value Reasoning

You are given a list of statements from Person A/B that express their values and preferences. You will use them to learn about Person A/B's general values and preferences systems. Then, you will be presented with several groups of new statements. Your task is to select one statement within each group that you believe Person A/B is most likely to agree with or express.

Person A Known Statements

- Family is not very important in my life
- I don't trust very much people I meet for the first time
- I disagree that science and technology are making our lives healthier, easier, and more comfortable
- The basic meaning of religion is to make sense of life in this world rather than after death

Person B Known Statements

- family is important in my life
- I somewhat trust people I meet for the first time
- I disagree that science and technology are making our lives healthier, easier, and more comfortable
- The basic meaning of religion is to make sense of life after death rather than in life

LMs' Predictions:

Person A/B will most likely to make the following statements...

Person A/B Predictions:

- I agree that whenever science and religion conflict, religion is always right
- Friends are more important than security
- I rarely attend religious services
- I trust very much my family

... Accuracy: 56%

Person A/B Predictions:

- I agree that whenever science and religion conflict, religion is always right
- I don't believe in life after death
- Friends are important in my life
- The society is better off because of science and technology

... Accuracy: 67%

Figure 1: INDIEVALUECATALOG, transformed from World Value Survey (WVS), contains statements expressing individualistic human values and preferences from 94K real humans worldwide. With this resource, we study LMs' ability to reason about individual human values.

Question (Phase 2: With Context)

What is the inconsistency in these parts of a scientific paper?

- The 'Original Question' uses a continuous 1-10 scale, but the 'Converted Statements' only group responses into four discrete ranges.
- The 'Original Question' defines 1 as 'Completely Dissatisfied' and 10 as 'Completely Satisfied', whereas the 'Converted Statements' redefine the lower numbers (1,2) as 'very satisfied' and the higher numbers (9,10) as 'very dissatisfied'.
- The 'Original Question' allows for open-ended 'Unstructured Survey Questions', while the 'Converted Statements' are limited to 253 pre-defined value-expressing statements, indicating a change in data type.
- The inconsistency lies in the 'LMs' Predictions' section, where Person A and Person B exhibit different accuracy percentages (56% vs 67%).

Next Question

Figure 21: Second part of survey interface showing question with *Focused Context*.

38

2052
2053
2054
2055
2056

Research Survey

2057 Question 6 of 10 - Phase 2

2058
2059

Context

2060
2061

PDF Document

2062
2063

For this question, you can scroll the whole paper PDF to answer.

2064
2065
2066
2067
2068
2069
2070
2071
2072
2073
2074
2075
2076
2077

[Open PDF Document](#)

💡 Pay attention to the following parts of the paper:

Text parts: From Line 371

Visual parts: Figure 2

2078
2079

Question (Phase 2: With Context)

2080
2081
2082
2083
2084
2085
2086
2087
2088
2089
2090
2091
2092
2093
2094
2095
2096
2097
2098
2099
2100
2101
2102
2103
2104
2105

What is the inconsistency in these parts of a scientific paper?

- The text claims that 'our model exhibits a more concentrated peak near $Q_{difference} = 0$ ', but Figure 2 shows 'normal_ours' having a main peak that is clearly more negative than CQL's main peak.
- Figure 2 illustrates that both models have their primary $Q_{difference}$ concentrations around positive values, which contradicts the text's statement that both models display a peak at negative $Q_{difference}$ values.
- The text states that CQL shows more spread in the positive $Q_{difference}$ direction, indicating more frequent overestimations, but Figure 2 clearly depicts that 'normal_ours' (the proposed method) has a more extensive and pronounced presence in the positive $Q_{difference}$ region compared to CQL.
- The text mentions that both models have a 'long tail extending toward positive values', but Figure 2 indicates that neither 'normal_cql' nor 'normal_ours' show any data points in the positive $Q_{difference}$ range.

[Next Question](#)

Figure 22: Third part of survey interface showing question with *Full Document Context*.